POLITECNICO DI TORINO

III Facoltà di Ingegneria(Ingegneria Dell'Informazione)

Corso di laurea in Igegneria Elettronica (Electronic Engineering)

A thesis submitted in partial fulfillment of the requirements for the degree of

Masters of Science in Electronic Engineering

Radio-Frequency Class J Amplifiers

IJSER

Supervisors:

Prof Giovanni Ghione

Prof Marco Pirola

Submitted by: Adolphus Nippae

April 12, 2011

- 1 -

Abstract

Recent advancements in the electronic communication request the need for high efficiency, as such there are needs for high efficiency wideband Radio Frequency Power Amplifier (RFPA) for future application in the communication industry. From the technological point of view, Gallium Nitride High Electrons Mobility Transistors (GaN HEMT) appear to be one of the most promising technologies, especially due to its capability for reduce size, resulting in minor weight and parasitic effects. On the other side, circuit design scientific community has shown an increasing interest in the Class J RFPA: it derives from the Class B RFPA, and in particular its implementation with GaN can be made useful to achieved wider bandwidth RFPA. In this framework, this thesis work has started from the Class J waveforms analysis. In order to achieve this task, theoretical basis of the Class J have been exploited and Matlab was used to analyze the waveforms of the Class J. To prove the equivalence of the Class J to the Class B in terms of performances, and aiming at using electronic components to prove the reality of this emerging device, Microwave Office (MWO) simulations were performed starting with an ideal model and passing on to more real structures.

Finally, after performing these analysis and simulations, the Class J was proven to have similar drain efficiency and output power to that of the Class B.

IJSER

- 2 -

ACKNOWLEDGEMENT

Firstly, my heartfelt gratitude's goes to the Politecnico di Torino (Polito) and the Government of the Republic of Liberia for granting me such bountiful opportunity to achieve this level of education. Also my appreciations to the International Office of Polito for its stewardship role during my stay at the Polito, most especially to Ms. Marina Rabagliati and her immediate staffs

Secondly, my gratitude goes to my mentors, Prof Giovanni Ghione and Prof Marco Pirola for granting me the opportunity to be one of the first to work on such an emerging device at the Politecnico di Torino. Also, my thanks and appreciations go to Dr. Roberto Quaglia for his tutorship role during the period of this project; he was always available when needed and was willing to share his technical know-hows with me.

Next, I would like to express thanks to my colleagues', Michele Tamagnone, Sharmin Aktar, Muhammad Awais, Jewel Okyere-Benya, Nosherwan Shoaib, Saeed Javidmehr, Alipourbabaie Zeinab and my Liberians friends at the Polito for their cordial working relationship during my stay at Polito.

Finally, my heartfelt gratitude goes to my uncle, Mr. J. Francis Nippae who started these million miles in 1980. Also, I am thankful to my friend and Church Brother, Mr. Daniel P. Dennis, Jr. who successfully took charged of my family during my study in Italy.

IJSER

TABLE OF CONTENTS

Abstract ..... - 1 -
ACKNOWLEDGEMENT ..... - 2 -
Chapter One ..... - 5 -
1.0 Introduction ..... - 5 -
1.1 Outline ..... - 5 -
1.2 Motivation ..... - 6 -
1.3 Project Goals ..... - 6 -
Chapter Two ..... - 6 -
2.0 RF Amplifier Theoretical Basics ..... - 6 -
2.1 A Generic Microwave RF Power Amplifier ..... - 7 -
2.2 Basic RF Power Amplifier Parameters ..... - 8 -
2.2.1 Efficiency and Power Added Efficiency ..... - 8 -
2.2.2 Linearity and Nonlinearity ..... - 9 -
2.2.3 FREQUENCY GENERATION ..... - 10 -
2.2.3.2 Harmonic Generation ..... - 13 -
2.2.4 Intermodulation Distortion ..... - 14 -
2.2.5 Adjacent Channel Interference ..... - 14 -
2.3 RF Power Amplifier Classes of Operations ..... - 15 -
2.3.1. Class B ..... - 17 -
2.4 HEMT Technology ..... - 20 -
2.4.1 The HEMT Transistors ..... - 20 -
GaAs, InP, GaSb, InAs, AlAs, GaP, GaN ..... - 22 -
2.4.2 Power Transistor Technologies for Communication Systems ..... - 22 -
2.4.3 GaN HEMT ..... - 23 -
Chapter Three ..... - 24 -
3.0 Class J Design approach ..... - 24 -
3.1 High Efficiency RFPA Design Approach ..... - 25 -
3.2 The Class J Concepts ..... - 27 -
3.3 Class J Essential ..... - 37 -

IJSER

Chapter Four .... - 40 -
4.0 Simulations and theoretical comparisons .... - 40 -
4.1 Simulations .... - 40 -
4.1.1 IV and Transcharacteristics Curves .... - 40 -
4.1.2 Schematics, Drain Voltage and Current Generation .... - 42 -
4.1.2.1 Class A .... - 43 -
4.1.2.2 Class B .... - 44 -
4.1.2.3 Class J .... - 45 -
4.2 Output Power and drain efficiency Comparisons .... - 46 -
4.3 Design with lumped element Resonators .... - 47 -
4.3.1 Class B .... - 47 -
4.3.2 Class J .... - 49 -
4.4 Class B Design – with lumped element biastee .... - 52 -
4.5 Parasitic element consideration – Class B. .... - 55 -
CHAPTER FIVE .... - 57 -
Conclusion .... - 57 -
APPENDIX .... - 58 -
Appendix A: Matlab codes for Class B RFPA .... - 58 -
Appendix B: Matlab codes for Class J Continuum voltage Waveforms .... - 59 -
Appendix C: Matlab codes for Class J RFPA .... - 61 -
Appendix D: Matlab codes for frequency spectrum .... - 62 -
REFERENCES .... - 64 -

IJSER

Chapter One

1.0 Introduction

This final project was entailed to gather theoretical basics and perform CAD base simulations for a high efficiency Radio Frequency Power Amplifier (RFPA) in the Class J . Basic Figures of Merit are evaluated: these include output power, efficiency, power added efficiency, voltage and current waveforms. During the tasks, calculus software Matlab was used to validate the theoretical analysis of the various waveforms, and the CAD and simulation suite Microwave Office (MWO) was used for verifying the expected performances adopting device non-linear models and passive circuit elements.

1.1 Outline

This final project began with a preparatory chapter with the objective of focusing on the fundamental and theoretical roots of radio frequency power amplifiers. Also in this chapter the transistor adopted, an High Electron Mobility Transistor (HEMT) was described. In the later chapter, the Class J RFPA theoretical basics were discussed; some of which include the generation of drain current and voltage equations and the fundamental and harmonic load equations were derived. Subsequently, the power harmonic components were generated aimed at comparing the DC power dissipated of the Class J with that of the Class B RFPA. Finally, chapter four was introduced to discuss the various simulations results. The simulations designs were lead employing a GaN HEMT device, using an available large signal model; its drain current and voltage characteristics were exploited. Aim at achieving the goal of this phase, an ideal mathematics model, the Santakluas was tuned to fit the DC I/V characteristics curves and trans-characteristics curve of the original GaN HEMT non-linear model. The obtained model was used to perform the simulations.

Final discussion will be given about the simulation results in comparison with theoretical expected performances.

IJSER

1.2 Motivation

To present, several RFPA applications, such as radar/satellite systems have not profited from advances in high power and high efficiency RF Amplifier due to their much wider RF bandwidth requirements. Also, power RF applications need higher gain and more power without complicated peripheral circuitry and that current and future nature of the RF market is being driven by the need for higher reliability, gain, linearity and output power requirements that will be constrained by the application's DC power supply limitations. Considering these challenges, the Class J RFPA was considered to be exploited for the future of the communication system developments or improvements. Also considering the advancement of the HEMT, that is relying on its high power output and high efficiency abilities and it capability to develop small devices, it was chosen as the model used for these investigations in the design of the Class J RFPA.

1.3 Project Goals

The goals of this project were geared toward gathering theoretical details of the Class J RFPA with some comparison to the widely adopted and well established Class B RFPA. It was aimed at deriving the drain current and drain voltage equations and generating their respective waveforms, with particular emphasis on the load impedance conditions that allow the generations of such waveforms. Finally, it was aimed at using a CAD tool, MWO/AWR to achieve desired parameters as gain, efficiency and designing input and output matching networks. In this framework, the analysis starts from a completely ideal circuit, and at every step real components are added for the observation of the causes of degradation in performances, always in comparison with the well-established Class B RFPA.

Chapter Two

2.0 RF Amplifier Theoretical Basics

As a Precursor for expanding into detail the project, this preparatory chapter is being introduced, focusing on the fundamental and theoretical roots of radio frequency power amplifiers. Key parameters and basic phenomena of RF power amplifier have been reviewed for

IJSER

the tasks ahead. Also the basis of the transistors model used, the HEMT technology and the GaN HEMT are being exploited for the task ahead.

2.1 A Generic Microwave RF Power Amplifier

A radio frequency power amplifiers (RFPA) in general and as it is discussed in this final project, basically consist of one or more active devices as the amplifying element(s) and a passive networks, that can contain both lumped and distributed elements connected the input and the output ports, as illustrated in Fig. 2.1

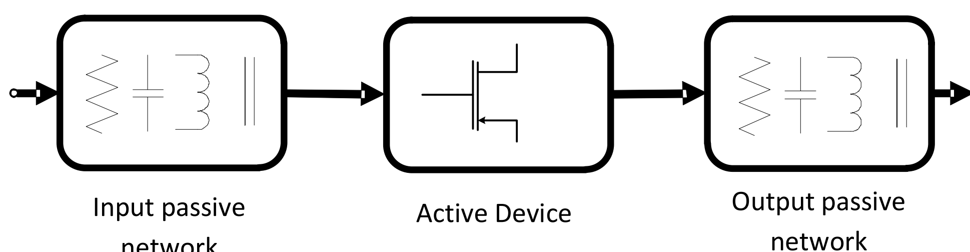

Figure 2.1: A generic single stage amplifier

IJSER

Active Device: The task of the active device is to amplify the input power signal by a constant factor. The device could be any type of transistor. In our case the GaN HEMT is being considered due to its high power output, efficiency and operating frequency capabilities. Design goal such as operating frequency, maximum collector/drain current, maximum output voltage and linearity establish the selection of the device type and quantity to be used. It is the cardiac of the PA, but it needs to be interfaced to the "external world" by passive networks for proper operation.

Passive Network: The designing of the passive input and output network is the vital part of the PA design. This network is responsible for filtering, stabilizing and wave shaping

2.2 Basic RF Power Amplifier Parameters

2.2.1 Efficiency and Power Added Efficiency

As related to the power and gain in microwave RF power amplifier, other parameters of interest are the efficiency, η and what is being considered as the power added efficiency, PAE. Considering the RFPA in figure 2.2:

$$P_{DC} = V_{DC} I_{DC} \tag{2.1}$$

Where, P_{DC} is the total DC power from the bias point and V_{DC} and I_{DC} are the DC voltage and current respectively. Thus the efficiency and PAE are given by,

$$\eta = \frac{P_{OUT}(f_0)}{P_{DC}} \tag{2.2}$$

and

$$PAE = \frac{P_{OUT}(f_0) - P_{IN}(f_0)}{P_{DC}} = \eta\left(1 - \frac{1}{G_{op}}\right) \tag{2.3}$$

IJSER

where, f_0 is the fundamental frequency, G_{op} the operational gain and P_{OUT} and P_{IN} are the output and input power respectively.

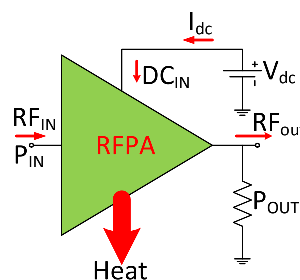

Figure 2.2: A typical RF Power Amplifier [5]

2.2.2 Linearity and Nonlinearity

Basically, all electronic circuits are nonlinear; this can be considered fundamentally real for all electronic circuits. The assumption which provides that most modern circuit theory is linear is practically only an approximation. There are circuits which have weak nonlinearity; thus causing those circuits to be used as linear circuit, as such nonlinearity become sources of phenomena that demean their systems performance. Thus, in such case nonlinearity should be minimized for better performance. Additionally, linear circuits are defined as those for which the superposition principle holds. Specifically, if excitations x_1 and x_2 are applied separately to a circuit having responses y_1 and y_2, respectively, the response to the excitation $ax_1 + bx_2$ is $ay_1 + by_2$, where a and b are arbitrary constants, which may be real or complex, time-invariant or time-varying. The later definition implies that the response of a linear, time-invariant circuit or system includes only those frequencies present in the excitation waveforms. Thus, linear, time-invariant circuits do not generate new frequencies.

IJSER

On the other hand, there are circuits which require high nonlinearity for better performance; the exploitations of nonlinearity bring into existence device like frequency multipliers. The problem of analyzing and designing such circuits is usually more complicated than for linear circuits; it is the subject of concern for this project. Contrary to linear circuits, nonlinear circuits generate additional new frequencies at other harmonics; this indicates some clear differences between linear and nonlinear circuits. Nonlinear circuits are often characterized as either *strongly nonlinear* or *weakly nonlinear*. A good working distinction is that a weakly nonlinear circuit can be described with adequate accuracy by a Taylor series expansion of its nonlinear current/voltage (*I/V*), charge/voltage (Q/V), or flux/current (ϕ/I) characteristic around some bias current or voltage. This definition implies that the characteristic is continuous, has continuous derivatives and for most practical purposes, does not require more than a few terms in its Taylor series [1].

If a circuit is weakly nonlinear, relatively straightforward techniques, such as power-series or Volterra-series analysis, can be used. Strongly nonlinear circuits are those that do not fit the

definition of weak nonlinearity; they must be analyzed by harmonic balance or time-domain methods. These circuits are not too difficult to handle if they include only single-frequency excitation or comprise only lumped elements. The most difficult case to analyze is a strongly nonlinear circuit that includes a mix of lumped and distributed components, arbitrary impedances, and multiple excitations. Additionally, we usually assume that the nonlinearities and RF drive are weak enough that the dc operating point is not perturbed. Virtually all transistors and passive components satisfy this definition if the excitation voltages are well within the components normal operating ranges [1].

2.2.3 FREQUENCY GENERATION

The traditional way of showing how new frequencies are generated in nonlinear circuits is to describe the component's I/V characteristic by a power series, and to assume that the excitation voltage has multiple frequency components. Figure 2.3 shows a circuit with excitation V_s and a resulting current, I. The circuit consists of a two-terminal nonlinearity, but because there is no source impedance, $V = V_s$ and the current can be found by substituting the source voltage waveform into the power series. Mathematically, the situation is the same as that of the transfer nonlinearity of Figure 2.3(b). The current is given by the expression

$$I = \mathrm{a}\mathrm{V} + bV^2 + cV^3 \tag{2.4}$$

where *a*, *b*, and *c* are constant, real coefficients. We assume that V_s is a two-tone excitation of the form

$$V_s = v_s(t) = aV_1(\omega_1 t) + bV_2(\omega_2 t) \tag{2.5}$$

Substituting (1.13) into (1.14) gives, for the first term,

$$i_a(t) = av_s(t) = aV_1 \cos(\omega_1 t) + aV_2 \cos(\omega_2 t) \tag{2.6}$$

IJSER

- 11 -

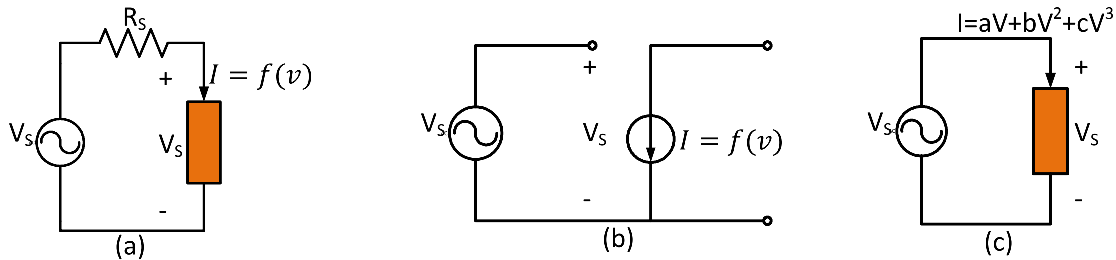

Figure 2.3: (a) Two-terminal nonlinearity; (b) transfer nonlinearity; (c) Two-terminal nonlinear resistor excited directly by a voltage source [1]

After doing the same with the second term, the quadratic, and applying the well-known trigonometric identities for squares and products of cosines, we obtain

$$i_b(t) = bv_s^2(t) = \frac{b}{2}\{V_1^2 + V_2^2 + V_1^2\cos(2\omega_1 t) + V_2^2\cos(2\omega_2 t)$$

$$+2V_1V_2[\cos((\omega_1+\omega_2)t) + \cos((\omega_1+\omega_2)t)]\} \quad 2.7)$$

IJSER

and the third term, the cubic, gives

$$i_c(t) = cv_s^2(t) = \frac{c}{4}\{V_1^3\, cos(3\omega_1 t) + V_2^3\, cos(3\omega_2 t)$$

$$+3V_1^2V_2[\cos((2\omega_1+\omega_2)t) + \cos((2\omega_1-\omega_2)t)]$$

$$+3V_1V_2^2[\cos((\omega_1+2\omega_2)t) + \cos((\omega_1-2\omega_2)t)]$$

$$+3(V_1^3 + V_1V_2^2)\cos(\omega_1\, t) + 3(V_2^3 + V_1^2V_2)\cos(\omega_2\, t) \quad (2.8)\ [1]$$

The total current in the nonlinear element is the sum of the current components in (2.6) through (2.8). This is the short-circuit current in the element; it consists of a remarkable

number of new frequency components, each successive term in (2.4) generating more new frequencies than the previous one; if a fourth- or fifth-degree nonlinearity were included, the number of new frequencies in the current would be even greater. However, in this case, there are only two frequency components of voltage, at ω_1 and ω_2, because the voltage source is in parallel with the nonlinearity. If there were a resistor between the voltage source and the nonlinearity, even more voltage components would be generated via the currents in that resistor, those new voltage components would generate new current components, and the number of frequency components would be, theoretically, infinite. In order to have a tractable analysis, it then would be necessary to ignore all frequency components beyond some point; the number of components retained would depend upon the strength of the nonlinearity, the magnitude of the excitation voltage, and the desired accuracy of the result.

A closer examination of the generated frequencies shows that all occur at a linear combination of the two excitation frequencies; that is, at the frequencies

IJSER

$$\omega_{m,n} = m\omega_1 + n\omega_2 \tag{2.9}$$

where $m, n = \cdots, -3, -2, -1, 0, 1, 2, 3, \ldots$. The term $\omega_{m,n}$, is called a *mixing frequency*, and the current component at that frequency (or voltage component, if there were one) is called a *mixing product*. The sum of the absolute values of m and n is called the *order* of the mixing product. For the m, n to be distinct, ω_1 and ω_2 must be *non-commensurate*; that is, they are not both harmonics of some single fundamental frequency. We will usually assume that the frequencies are non-commensurate when two or more arbitrary excitation frequencies exist.

An examination of (2.6) through (2.8) shows that a kth-degree term in the power series (2.4) produces new mixing frequencies of order k or below; those mixing frequencies are k^{th}-order combinations of the frequencies of the voltage components at the element's terminals. This does not, however, mean that $m + n < k$ in every nonlinear circuit. In the above example, the

terminal voltage components were the excitation voltages, so only two frequencies existed. However, if the circuit of Figure 2.3 included a resistor in series with the nonlinear element, the total terminal voltage would have included not only the excitation frequencies, but higher-order mixing products as well. The nonlinear element then would have generated all possible k^{th}-order combinations of those mixing products and the excitation frequencies. Thus, in general, a nonlinear element can generate mixing frequencies involving all possible harmonics of the excitation frequencies, even those where $m+n$ is greater than the highest power in the power series. It does this by generating k^{th}-order mixing products between all the frequency components of its terminal voltage. Another conclusion one may draw from (2.6) through (2.8) is that the odd-degree terms in the power series generate only odd-order mixing products, and the even-degree terms generate even-order products. This property is exploited by balanced structures. Balanced circuits combine nonlinear elements in such a way that either the even- or odd-degree terms in their power series are eliminated, so only even- or odd-order mixing frequencies are generated. These circuits are very useful in rejecting unwanted even- or odd-order mixing frequencies [1].

IJSER

2.2.3.2 Harmonic Generation

One noticeable property of a nonlinear system is its generation of harmonics of the excitation frequency or frequencies. These are evident as the terms in (2.6) through (2.8) at $m\omega_1,\ m\omega_2$. The mth harmonic of an excitation frequency is an mth-order mixing frequency. In narrow-band systems, harmonics are not a serious problem because they are far removed in frequency from the signals of interest and inevitably are rejected by filters. In others, such as transmitters, harmonics may interfere with other communications systems and must be reduced by filters or other means.

2.2.4 Intermodulation Distortion

All the mixing frequencies in (2.6) through (2.8) that arise as linear combinations of two or more tones are often called *intermodulation* (IM) *products*. IM products generated in an amplifier or communications receiver often present a serious problem, because they represent spurious/counterfeit signals that interfere with, and can be mistaken for, desired signals. IM products are generally much weaker than the signals that generate them; however, a situation often arises wherein two or more very strong signals, which may be outside the receiver's passband, generate an IM product that is within the receiver's passband and obscures a weak, desired signal. Even-order IM products usually occur at frequencies well above or below the signals that generate them, and consequently are often of little concern. The IM products of greatest concern are usually the third-order ones that occur at $2\omega_1 - \omega_2$ and $2\omega_2 - \omega_1$, because they are the strongest of all oddorder products, are close to the signals that generate them, and often cannot be rejected by filters. Thus, intermodulation is a major concern in microwave systems.

IJSER

2.2.5 Adjacent Channel Interference

In many communications systems, especially those used for cellular telephones and other forms of telecommunications, modulated signals are squeezed into narrow, contiguous channels. Nonlinear distortion can generate energy that falls outside the intended channel. This is called *adjacent-channel interference*, *spectral regrowth*, or sometimes *co-channels interference*. Adjacent-channel interference is fundamentally odd-order intermodulation distortion, and, like most odd-order IM, it is dominated by third-order effects, although higher-order nonlinearities may also contribute.

- 15 -

2.3 RF Power Amplifier Classes of Operations

In this section, short theoretical and operational basics of class B of amplifier are being examined, indicating the source and tradeoff for the amplifier class of concern, the class J RF power amplifier. Amplifiers are basically specified according to their input and output properties and sometimes with their operational period or conduction angle. All the analyzed classes of power amplifier has common basic topology that includes an active device with DC bias feeders and an output matching network as shown in Figure 2.4, but the drain/collector voltage and current waveforms change with classes. They differ by the method of operation and harmonic frequency content. The efficiency and linearity are strongly affected by these conditions. These classes of amplifier can be classified into two major types, the transconductance amplifiers, (Classes A, AB, B and C) and the switching amplifiers (Classes D, E and F) referred to as high efficiency amplifiers. There are others classes (i.e. G, H) of RF power amplifier as mentioned in [2][6].

IJSER

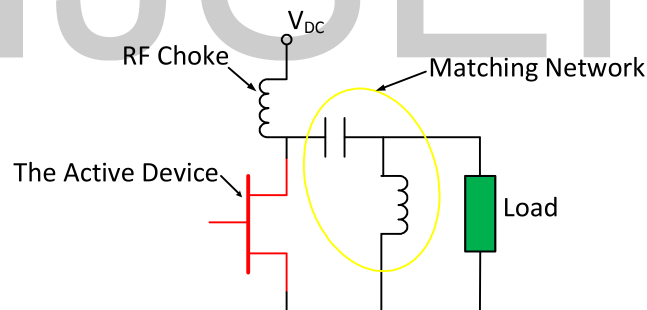

Figure 2.4: A generic power amplifier indicating both active device and output

Tuned load circuit is used as a means of reducing distortion on the power amplifier output stage. The tuned load resonates at desired frequency; as a result a desired sinusoidal waveform is generated at the output. The main difference among class A, B, AB and C is the conduction angle (θ) of the rain/collector current; figure 2.5 illustrates this difference, indicating their respective waveforms and conduction angle. Key parameters are shown in table 2.1.

Table 2.1: Traditional PA Classes parameters Variations			
RFPA Classes	Conduction angles	Drain Efficiency, η (%)	Power Output Potential
A	$\theta=2\pi$	50	Large
B	$\theta=\pi$	78.5	Medium
AB	$0 \rightarrow 2\pi$	$50<\eta< 78.5$	Medium
C	$0<\theta<\pi$	100	Low

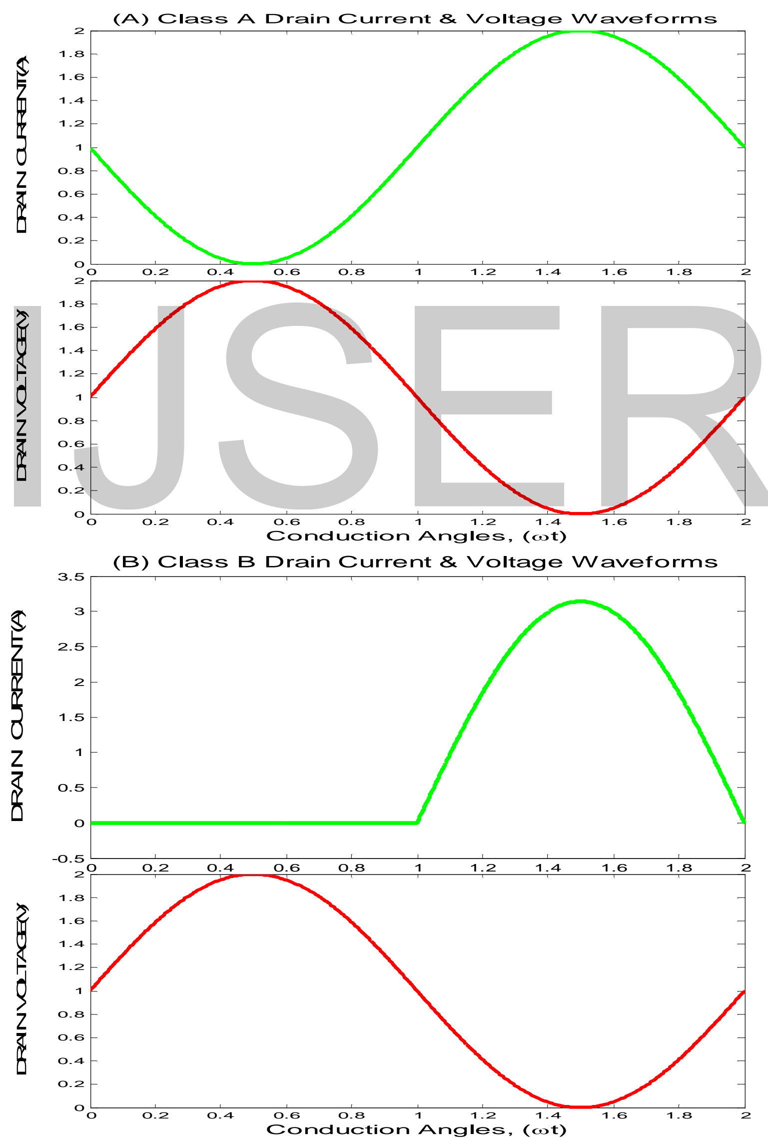

IJSER

Figure 2.5(A&B): Ideal traditional RF Power Amplifier Waveforms, (A) Class A ($\theta=2\pi$), Class B ($\theta=\pi$)

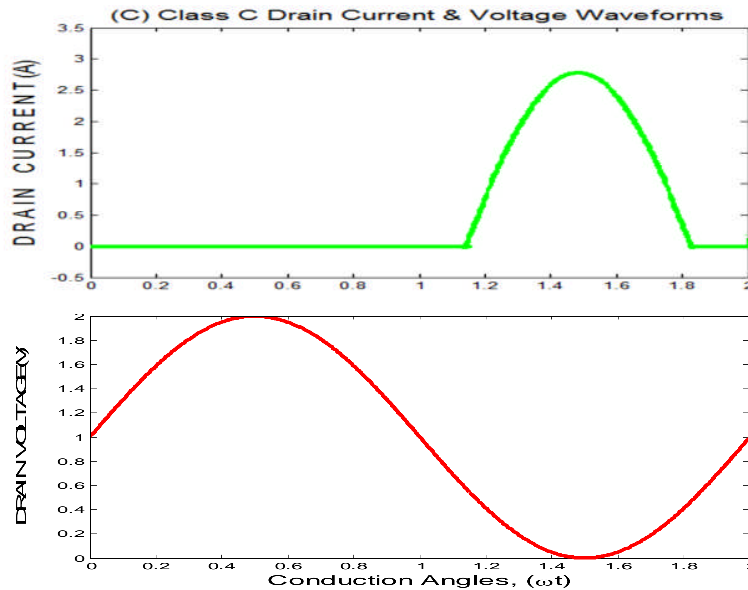

Figure 2.5(C): Ideal traditional RF Power Amplifier Waveforms, (C) Class C (0<θ<π)

IJSER

2.3.1. Class B

The class B power amplifier conducts for 50% of the period of its input signal, which means a conduction angle $\alpha = 180^o or\ \pi$. As such, Class B amplifiers only amplify half of the input wave cycle, thus creating a large amount of distortion, but their efficiency is greatly improved and is much better than Class A: the distortion is reduced applying a resonator at the output (tuned load Class B) or using a combined amplifier with the devices working in anti-phase (push pull). The maximum theoretical efficiency of Class B is about 78.5% (i.e., π/4). This high efficiency is the result of the amplifying device being switched off completely during half of its conduction time, thus causing low power dissipation. Figure 2.6 illustrates typical wave forms as applied in Class B PA.

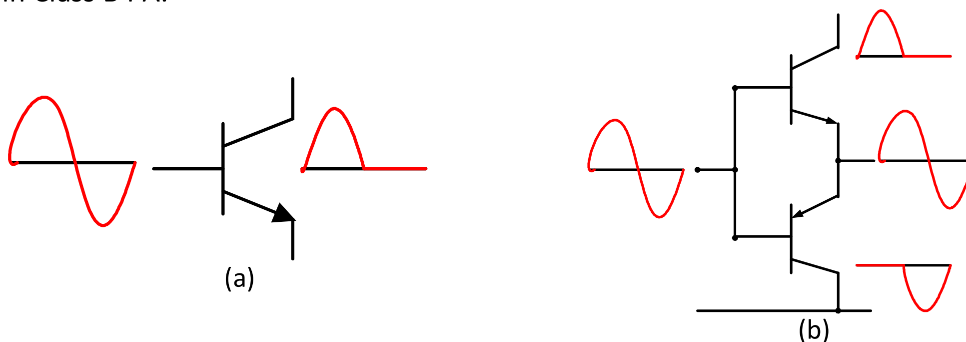

Figure 2.6: Class B active device(S) and waveforms, (a) Single active device stage; (b) Push-Pull stage [3]

For the push-pull case, these amplifiers are subject to *crossover distortion* if the transition from one active element to the other is not perfect, as when two complementary transistors (i.e., one PNP, one NPN) are connected as two emitter followers with their base and emitter terminals in common, requiring the base voltage to slew across the region where both devices are turned off [3].

Gearing at illustrating the behavior of class B voltage and current waveforms, let's consider a Class B PA with tuned load as depicted figure 2.4. In this situation, for the tuned load, there is an open at the fundamental frequency, f_0 and shorted at all other frequency above and below the fundamental frequency. The gate voltage swings below threshold for 50% of the period, above for the other 50% and due to the load is tuned, only the fundamental component gets to the load resistor; the DC component is blocked by the capacitor included or in series with the bias T.

IJSER

As earlier mentioned, the Class B is bias in such a way that the transistor only conduct during half of its RF cycle; the expansion of its drain current is a half-sine waveform and its drain voltage is a full sine waveform. The both waveforms over lap at a less amplitude, thus producing less power dissipation, which gear toward it high drain efficiency; figure 2.7 shows the overlapping in the waveforms. See appendix A for Matlab codes that generate these waveforms. The Class B drain current and voltage waveforms equation can be expressed as the following as indicated in [4].

$$v_D(\theta) = V_{ds} - V_0 \sin\theta$$

$$i_D(\theta) = I_0 \sin\theta\,,\ 0 \le \theta \le \pi$$

$$= 0, \qquad \pi \le \theta \le 2\pi$$

The half-sine waveform of the drain current is given by:

$$i_D(\theta) = I_0 \left[\frac{1}{\pi} + \frac{1}{2}\sin\theta - \frac{2}{\pi}\sum_{n=2,4,6,\dots}\frac{1}{n^2-1}\cos n\theta\right]$$

- 19 -

Where $I_0 = I_{max}\ or\ I_{peak}\ and\ V_o = V_{max}$ the neutralizing the DC current gives:

$$i_D(\theta) = 1 + \frac{\pi}{2}\sin\theta - 2\sum_{n=2,4,6,\dots}\frac{1}{n^2-1}\cos n\theta$$

This implies that the maximum DC current is 1A.

Given the above, we can formulate expressions for the DC and fundament components for the drain voltage drain current for the Class B, so as to define its efficiency and other properties.

$$I_{dc} = \frac{I_{peak}}{\pi}\ and\ V_{dc} = \frac{V_{max}}{2} \xrightarrow{yields} P_{dc} = V_{dc}I_{dc} = \frac{V_{max}I_{peak}}{2\pi}$$

$$I_{fund} = \frac{I_{max}}{2}\ and\ V_{fund} = \frac{V_{max}}{2} \xrightarrow{yields} P_{out} = \frac{1}{2}V_{fund}I_{fund} = \frac{1}{8}V_{max}I_{peak}$$

Thus given the Class B maximum theoretical efficiency to be 78.54% as earlier mentioned and expressed below:

$$\eta = \frac{P_{out}}{P_{dc}} = \frac{\pi}{4} \cong 78.54\%$$

Aiming at comparing the Class B output impedance with that of the Class J output impedance; in other to obtain optimum load, the Class B load impedances can be computed from the original drain current and drain voltage equations as seen bellow:

$$Z_{fundamental} = \frac{V_{fundamental}}{I_{fundamental}} = \frac{V_0\sin\theta}{I_0\sin\theta} = \frac{V_{max}}{I_0} = \frac{2(V_{dc} - V_{knee})}{I_{max}}$$

$$\xrightarrow{yields} Z_{L_f} = R + j0$$

$$Z_{fundamental} = \frac{V_{fundamental}}{I_{fundamental}} = \frac{V_0\sin\theta}{\frac{\pi I_0}{2}\sin\theta} = \frac{V_{max}}{\frac{\pi I_{max}}{2}} = \frac{2V_{max}}{\pi I_{max}}$$

$$Z_{2nd\ harm} \xrightarrow{yields} 0 \underset{implies}{\Longrightarrow} short\ @\ all\ harmonic$$

Thus, expression the Class B RFPA fundamental impedance in standard form gives,

$$Z_{fundamenatl} = R + j0$$

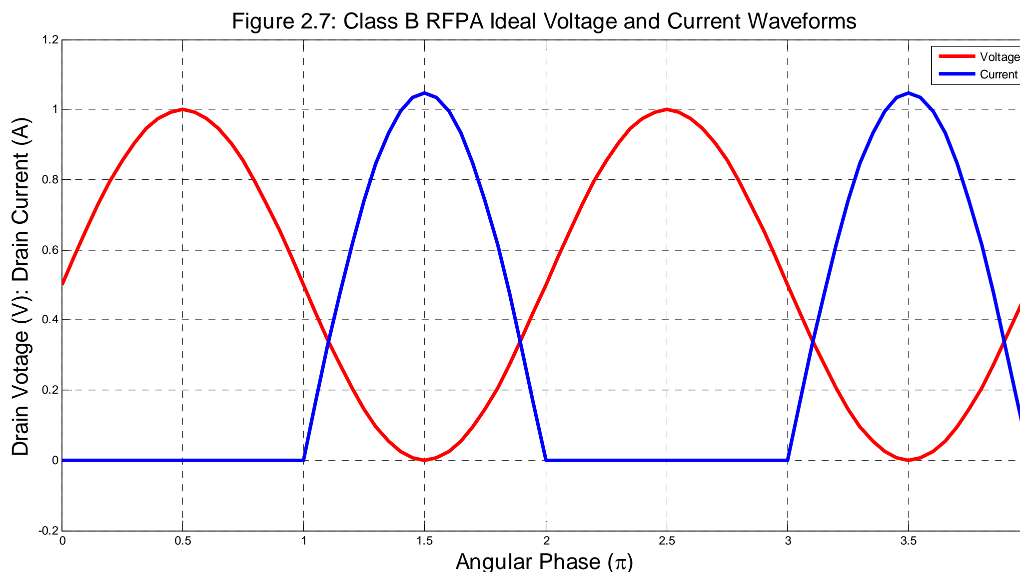

Figure 2.7: Class B RFPA Ideal Voltage and Current Waveforms

2.4 HEMT Technology

In this chapter, the properties and theoretical basis of the High Electron Mobility Transistors (HEMT) and the transistor model used for this design, the Gallium Nitride HEMT (GaN HEMT) are examined for the enhancement of design work ahead. Also the advantage(s) of HEMT over its competitors, basically the Laterally Diffused Metal Oxide Semiconductor (LDMOS) as it is related to base station operation in communication system are being examined. The success of the HEMT came about as the result of the

IJSER

inventor, Mimura, failure to develop the accumulation-type, GaAsMOSFET; detail of HEMT history can be found in [18].

2.4.1 The HEMT Transistors

High electron mobility transistor (HEMT), also known as heterostructure FET (HFET) or modulation-doped FET (MODFET), is a field effect transistor incorporating a junction between two materials with different band gaps (i.e., a heterojunction) as the channel instead of a doped region, as is generally the case for MOSFET. A commonly used material combination is GaAs with AlGaAs though there is wide variation, dependent on the application of the device. In recent years, Gallium Nitride HEMTs have attracted attention due to their high-power performance [15]. Figure 3.1 shows a tropical conventional structure of HEMT

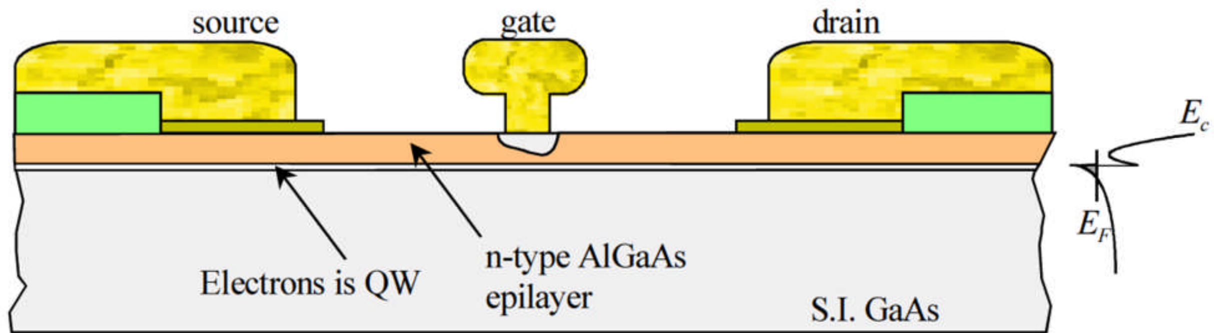

Figure 2.8: Conventional HEMT Structure [16]

The heart of a HEMT is the heterojunction between a barrier layer consisting of one semiconductor grown on a channel layer composed of another semiconductor. For proper HEMT operation the conduction band of the barrier layer must be located at a higher energy level than the conduction band of the channel layer. If this condition is fulfilled, a two-dimensional electron gas (2DEG) which constitutes the transistor's channel is formed at the heterojunction [16].

IJSER

HEMT based on the III-V semiconductors (grouping of element and compounds semiconductor for RF and microwave devices are shown in table 3.1), GaAs and InP are very popular and successful devices for radio frequency applications. The operating frequencies of these transistors cover the range from 800 *MHz* to 100 GHz [16].

Table 2.2 [15]	
Group	**Element/Compounds**
III-V	**GaAs, InP, GaSb, InAs, AlAs, GaP, GaN**
II-IV	**CdTe HgTe ZnS CdSe**
IV-IV	**SiC, SiGe**
IV	**SI**

Properties

Widegap (>2eV) → high power

Narrowgap (<1eV) → low noise

General purpose element & compound

Group used for this project

IJSER

2.4.2 Power Transistor Technologies for Communication Systems

RF Power transistors are used for RF Power Amplification in numerous applications from point-to-multipoint communications to Radar. Of particular interest, due to the need of high power, is the market of base stations for mobile communications. Performances of RF power amplifiers for base station transceivers results in a tradeoff between linearity, high power output, efficiency and gain. Since the 2000s there have been tremendous improvements in the electronics communication industries ranging from telecommunication to satellite/radar communications gearing toward these tradeoffs. These advancements have been as the result of developing devices with high output power level, higher efficiency, etc. of the transistor devices used, basically LDMOS, High voltage MESFETs, HBTs, and AlGaN/GaN HEMT, the later. In comparison to the conventional gate transistors, the field plate (FP) MESFET/HEMTs has increased breakdown voltage and increased gate capacitance. Therefore, the power density and operating voltage of the FP transistors are higher [4]. Different high power transistors

show different performance parameters at different frequency. Table 3.2 shows different performance of serious of these high power transistor operations at a given frequency; a ceramic package of transistor's performance at 2GHz.

Table 2.3: Ceramic package transistor's performance at 2.1GHz [4]

Device	Typical break Down voltage (V)	Operating Voltage (V)	Output Power (W)	Gain (dB)	Efficiency
Si BJT	63	36	110	7.4	40
Si LDMOS	70	28	100	13	55
GaAs FP- MESFET	60	28	300	14	63
SiC MESFET	90	40	56	10	55
GaAs FP- pHEMT	50	26	43	11.5	56
SiC GaN HEMT	80	48	370	10	50
GaAS HBT	70	28	20	11	70

IJSER

2.4.3 GaN HEMT

As mentioned in [13], the GaN base transistors have received increased attention because of their great potential for high-voltage power applications such as cellular phone base station systems. This potential is attributed to the high breakdown field (~$3x10^6$V/cm) and the strong piezoelectricity leading to a high carrier density in a $10^{13}cm^{-2}$ ranges. Also, a peak drift velocity exceeding $2x10^7$cm/s makes GaN transistors very attractive for millimeter-wave applications such as wireless internet access systems. Additionally, for all high-data-rate communication applications, device linearity is a key performance specification. Due to their large operation space in the I-V plane as compared to the lower band-gap semiconductors, GaN-based HEMTs

have the potential to offer high linearity for the stringent requirements. The linearity criteria for high power transmitters are usually expressed in terms of associated output power and efficiency at a certain distortion level [19].

The advantages of the HEMT include its high carrier concentration and its higher electron mobility due to reduced ionized impurity scattering. The combination of high carrier concentration and high electron mobility results in a high current density and a low channel resistance, which are especially important for high frequency operation and power switching applications.

From the amplifier point of view, GaN-based HEMTs have many advantages over existing production technologies (e.g. GaAs). The high output power density allows the fabrication of much smaller size devices with the same output power. Higher impedance due to the smaller size allows for easier and lower loss matching in amplifiers. The operation at high voltage due to its high breakdown electric field not only reduces the need for voltage conversion, but also provides the potential to obtain high efficiency, which is a critical parameter for amplifiers. The wide bandgap also enables it to operate at high temperatures. At the same time, the HEMT offers better noise performance than that of MESFET's [19].

IJSER

Chapter Three

3.0 Class J Design approach

In this chapter, the general concepts of designing high efficiency RF power amplifier are being exploited, followed by comprehensive design topology on the main RFPA class under discussion for this paper, the Class J RFPA. The definition, principles of operation, basic waveforms, efficiency of the Class J are being considered.

- 25 -

3.1 High Efficiency RFPA Design Approach

In the design of high efficiency RFPA, basically two main approaches are commonly employed, nonlinear device models and load-pull measurements. The nonlinear device models uses CAD environment and allows the observation and optimization of current and voltage waveforms. However, this design approach relies heavily on the accuracy of the nonlinear device model and any discrepancies between the measurements and simulations render the simulated waveforms unreliable. Load-pull measurements are more practical for low efficiency designs which utilize only the fundamental frequency; large number of combinations between the harmonic loads required for high efficiency designs would lead to prohibitively long sweep times [7]. Very often a mixed solution is adopted: limited regions of the Smith Chart for the optimum load are identified by large signal model simulations, and then a load pull measure is carried to accurately identify the harmonic terminations.

IJSER

As such, in the design of RF power amplifier one key issue of concern is the improvement of *drain efficiency*, that's the fundamental power divided by the dc dissipated power as expressed below:

$$\eta_{drain\ eff} = \frac{P_{fund}}{P_{dc}} \quad (3.1)$$

Considering the above formula, in order to improve the drain one should increase the fundamental power (all power should be at the fundamental and there should be no power dissipated at the higher order harmonics) or decrease the dc dissipated power on the device. The dc dissipated power is defined as:

$$P_d = \frac{1}{T}\int I_{ds}V_{ds}dt \quad (3.2)$$

Thus, in order to decrease P_d the product of the drain current and voltage should be minimized; also the waveforms of the drain current and voltage should intercept at very low points (i.e., $I_D = V_D = 0$). As such there will be no power dissipated at output of the device; this idea will be applied to the Class J as we proceed in our design work.

- 26 -

Figure 3.1(a & b) show ideal waveforms for the trans-conductor amplifiers (B & AB) and the switching power amplifiers respectively.

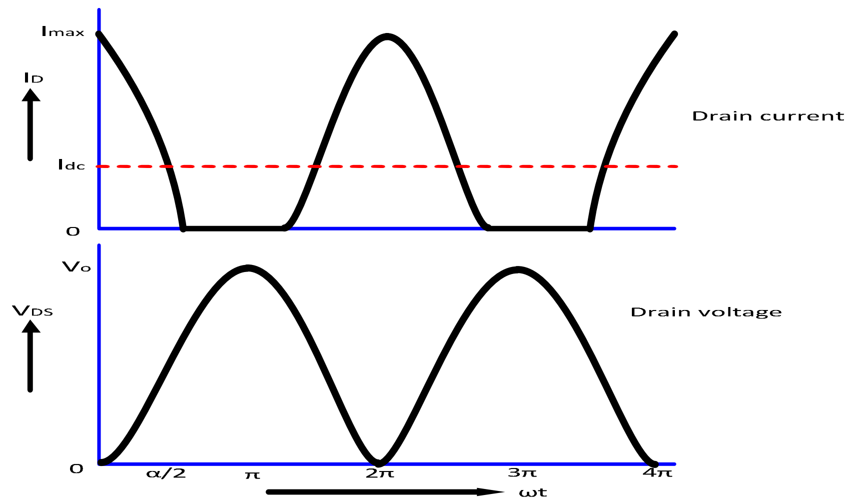

Figure 3.1(a): Ideal Class B & AB drain current and voltage waveforms

IJSER

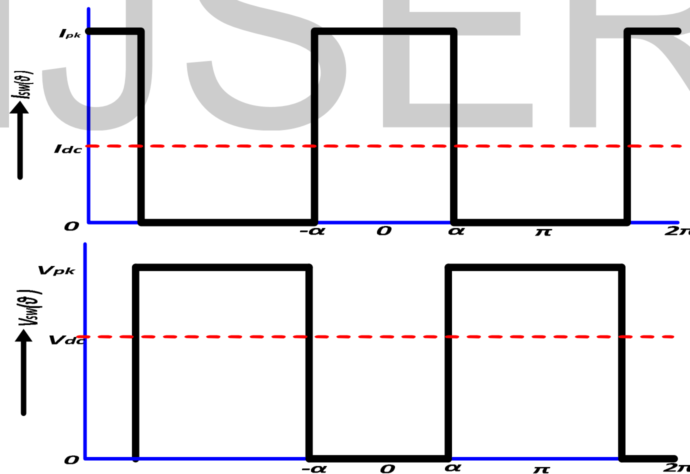

Figure 3.1(b): Ideal switching RFPA drain current and voltage

As presented in figure 3.1 (a & b), it can be seen that there exist concurrently drain current and voltage in the traditional amplifier (figure 3.1a) during its operational period, thus causing power dissipation in these classes, whereas, the positive exist for the ideal switching amplifiers (figure 3.1b), thus leading to high efficiency and performance for these classes. Accordingly,

similar approach will be used to gear at the Class J design, except that it operates in the efficiency range of the Class B but with a more easily attainable circuit.

3.2 The Class J Concepts

The Class J RFPA is an emerging class of high efficiency and low power dissipation radiofrequency power amplifier undergoing study at many academic and technical RF design institutions. This class of amplifier was proposed by Steve C. Cripps as indicated in his book [2] The definition of the Class J is to simply consider fundamental and second harmonic termination; the drain current can be manipulated (amplitude variations and applying some shifting to the phase) to obtain the drain voltage [11], the newly achieved drain voltage waveform must be something like that of a half sine wave, almost like that of the current waveform. Also to achieve the drain voltage, we can also consider second harmonic termination to the general high efficiency RFPA voltage waveform as described in [9]. In [9] the authors referred to this voltage waveform equation as "New Formulation of PA Voltage Waveform", this same equation was also used by Cripps in [8]; the expression for this waveform is indicated below:

IJSER

$$V(\theta) = V_{dc} - V_{1r}\cos\theta - V_{1q}\sin\theta \sum_n V_{nq}\sin n\theta \qquad (3.4)$$

Where V_{dc} represents the DC supply voltage, detail of this expression is better described in [9].

From equation 3.4 and as described in [9], the Class J RFPA drain voltage waveform can be expressed as shown in equation 3.5 by considering normalized $V_{dc}\ and\ V_{1r}$, the fundamental and the second harmonic termination formation as described in [2],

$$v_j(\theta) = 1 - \cos\theta - \sin\theta + \frac{1}{2}\sin 2\theta \qquad (3.5)$$

Where $v_j(\theta)$ represents the Class J drain voltage at a conduction angle, θ; after some mathematical manipulations, (i.e., applying trigonometry functions and factorizing), it was deduced to the below expression:

- 28 -

$$v_j\,(\theta) = (1 - \cos\theta)(1 - \sin\theta) \quad (3.6)[9]$$

The equation (3.6) evidently guarantees the conditions expressed in (3) & (4) of [9], that which provides that $\theta = 0$ should be met. "From this observation, it follows that there exists a family of such expressions based on the product of factors having the form" [9]:

$$v_j\,(\theta) = (1 - \beta\cos\theta)(1 - \alpha\sin\theta),\ (-1 < \alpha < 1,\ 0 < \beta < 1) \quad (3.7)[9]$$

As such families of the Class J voltage waveforms are plotted in figure 3.2; see appendix B for Matlab codes that generate these waveforms. As depicted in the continuum plot of the Class J voltage waveform, we will consider the family of $0.85 \leq \alpha \leq 1$, in describing the Class J drain current and drain voltage waveforms phenomena; these yield similar results as we will see later in the next analysis.

IJSER

Also as illustrated in figure 3.2, the family containing $-0.5 \leq \alpha \leq 0.5$, show not a considerable change in the drain voltage waveform as relates to its counterpart, the class B drain voltage waveform; basically at $\alpha = 0$, we see purely that of the Class B drain voltage waveform.

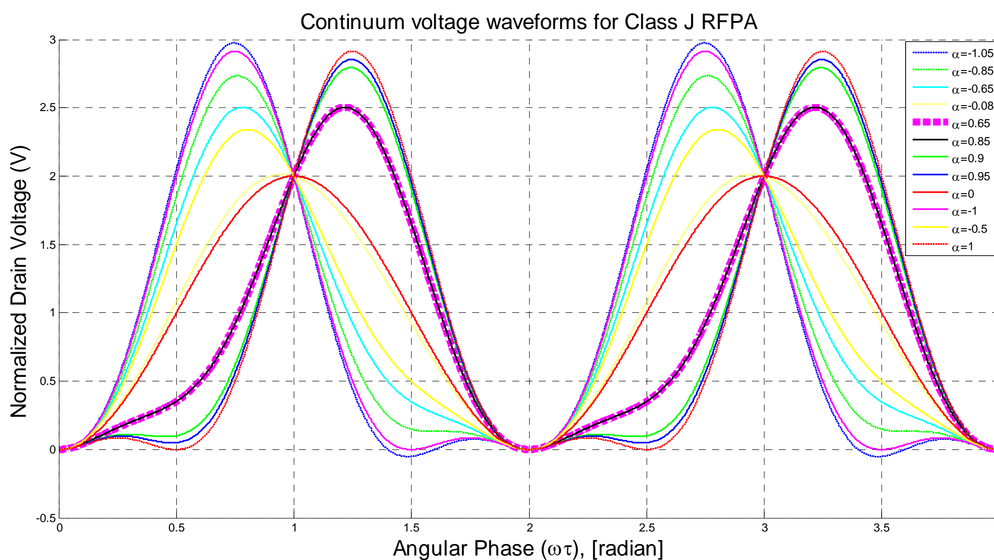

Figure 3.2, Continuum of theoretical voltage waves, Class J*, thru Class B, to Class J (β =1, in all cases)

Aim at describing other parameters of the Class J RFPA; we used the manipulation of the drain current waveform to generate the drain voltage waveform as earlier discussed in this chapter. In chapter two, the half sine wave drain current for the Class B was described as having the form,

$$i_D(\theta) = I_{dc}(1 + \frac{\pi}{2}\sin\theta - 2\sum_{n=2,4,6,\dots}\frac{1}{n^2-1}\cos n\theta) \quad (3.8)$$

Where I_{dc} equals $\frac{I_{peak}}{\pi}$ and n represents the even harmonics. Gearing at the class J concept, the drain current should contain a DC, fundamental and second harmonic components only, thus reducing the equation (3.8) to (3.9), which can be referred to as the Class J drain current.

$$i_{Dj}(\theta) = I_{dc}(1 + \frac{\pi}{2}\sin\theta - \frac{2}{3}\cos 2\theta) \quad (3.9)$$

Oops! The Class J current has similar shape like that of the Class B current waveform; figure 3.3 shows this waveform. As seen in (3.9), we considered that the Class J waveforms has only three components

$$i_{Dj}(\theta) = I_{dc} + I_{fundamental} + I_{2nd\ harmonic}$$

Thus, neutralizing I_{dc}, we can say that,

$$I_{dc} = 1$$

$$I_{fundamenatl} = \frac{\pi}{2}\sin\theta$$

$$I_{2nd\ harmonic} = -\frac{2}{3}\cos 2\theta$$

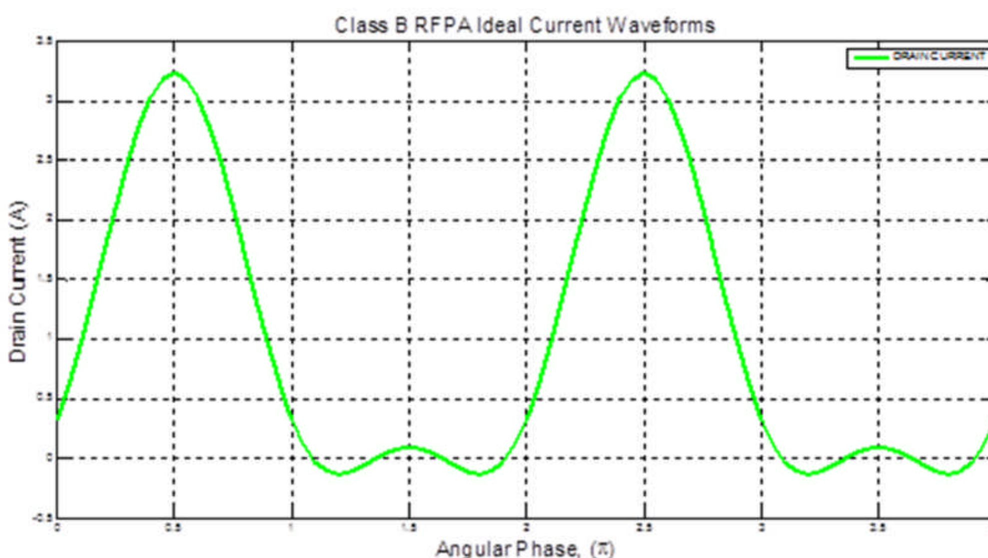

Figure 3.3: Ideal waveform for Class J RF Power Amplifier

IJSER

Now that we have an indication of the current equation, we can generate the voltage equation by manipulating the current equation [11]. This will lead us to achieving the loads and others parameters of the Class J; considering that we need high efficiency amplifier, we need to have no or very DC less power dissipated at the output. This means that we should have a completely reactive terminated load.

Considering that both the drain current and voltage are like an half sine wave, we can manipulate the equation generated for the drain current; the voltage should have different amplitude at both fundamental and second harmonic and considering the kind of reactive load termination at the fundamental and second harmonic we have shifting in the waveform. Thus, considering the drain current equation, we can generate an equation for the drain voltage, V_{Dj}, having the form

$$V_{Dj}(\theta) = V_{dc}\{1 + A\sin(\theta + \alpha) - B\cos(2\theta + \beta)\} \quad (3.10)$$

Where $A \& B$ represent the respective amplitude of the fundamental and second harmonic and $\alpha \& \beta$ represent their respective phase shift. Neutralizing V_{dc} and since the phase are based on the kind of reactive termination, let's ignore the phase shifts, considering the drain voltage ordinarily as

$$V_{ODj}(\theta) = 1 + A\sin\theta - B\cos 2\theta \quad (3.11)$$

As represented in equation 3.11, we can apply some mathematical manipulations (trigonometry and differentiation) to obtain maximum and minimum values for $A \& B$. From (3.11) we obtained,

$$V_{ODj} = 1 + A + B \qquad @\, \theta = \theta_1 = \frac{\pi}{2}$$

$$V_{ODj} = 1 - A + B \qquad @\, \theta = \theta_2 = \frac{3\pi}{2}$$

$$V_{ODj} = 1 - B \qquad @\, \theta = \theta_3 = \pi \;\&\; \theta = \theta_4 = 2\pi$$

Differentiating (3.11) and equate it to zero, we obtained:

$$V'_{ODj} = A\cos\theta + 2B\sin 2\theta = 0 \quad (3.12)$$

$$V'_{ODj} = A\cos\theta + 4B\sin\theta\cos\theta = 0$$

- 31 -

$$V'_{ODj} = \cos\theta\,(A + 4B\sin\theta) = 0 \tag{3.12'}$$

Thus, from (3.12'), for a true and necessary conditions, $\theta \in \left\{\frac{\pi}{2}, \frac{3\pi}{2}, \sin^{-1}(-\frac{A}{4B})\right\}$. As such we can obtain minimum values for V_{ODj}, by adding and subtracting $\sin^{-1}(-\frac{A}{4B})$ from θ_4 & θ_3 respectively. So, applying (3.11) for $\theta'_3 = \pi - \sin^{-1}\left(-\frac{A}{4B}\right)$ and $\theta'_4 = 2\pi + \sin^{-1}\left(-\frac{A}{4B}\right)$ we obtained

$$V_{ODjmin} = A\sin\left[\sin^{-1}(-\frac{A}{4B})\right] - B\cos\left[2\sin^{-1}(-\frac{A}{4B})\right] \tag{3.13}$$

We want the minimum value for V_{Dj} to be zero, so we equate equation 3.13 to zero, thus obtaining minimum values for the drain voltage by applying trigonometric functions (Compositions of trigonometry and inverse trigonometry functions) and little algebra. The resulting manipulation gives:

$$V_{ODjmin} = 1 - B + A\left(\frac{A}{4B}\right) - 2B\left(\frac{A}{4B}\right)^2 = 0 \tag{3.14}$$

$$= 1 - B + \frac{A^2}{8B} = 0 \xrightarrow{yields} B = \frac{1}{2} \pm \frac{1}{2}\sqrt{1 - \frac{A^2}{2}} \tag{3.14'}$$

IJSER

Thus, from equation 3.14' we can obtain maximum value for "A" and minimum value for "B".
As seen in (3.14'), the argument of the radical must be greater than or equals zero, so we have

$$1 - \frac{A^2}{2} \geq 0 \xrightarrow{yields} A \leq \sqrt{2} \xrightarrow{yields} A_{max} = \sqrt{2} \xrightarrow{yields} B_{min} = \frac{1}{2}$$

$$\xrightarrow{yields} A_{min} = 0 \xrightarrow{yields} B_{max} = 1$$

Considering that we are interested in higher efficiency device, we chose

$$A_{max} = \sqrt{2}\ \ and\ B_{min} = \frac{1}{2} \tag{3.15}$$

Substituting equation 3.15 into 3.10 gives,

$$V_{Dj}(\theta) = 1 + \sqrt{2}\sin(\theta + \alpha) - \frac{1}{2}\cos(2\theta + \beta) \tag{3.16}$$

Next we load the second harmonic with a capacitive load $\left(\beta = \frac{\pi}{2}\right)$, thus causing the second harmonic voltage to lead the second harmonic drain current by 90^0. Also, at the fundamental, the drain voltage should be lagged by 45^0 $(\alpha = \frac{\pi}{4})$, in order to synchronize the maximum amplitude of the fundamental with that of the second harmonic. Finally, we obtained the Class J drain voltage to be as shown:

$$V_{Dj}(\theta) = V_{dc}\left\{1 + \sqrt{2}\sin\left(\theta + \pi + \frac{\pi}{4}\right) - \frac{1}{2}\cos\left(2\theta + \pi - \frac{\pi}{2}\right)\right\} \quad (3.17)$$

Figure 3.5 shows the drain voltage waveform with respect to its angular phase, something like that of the half sine wave; indeed, this is what we wanted. The 180^0 is due to the reverse phase shift in the drain voltage and drain current; this can be seen as indicated in figure 3.6 and 3.7.

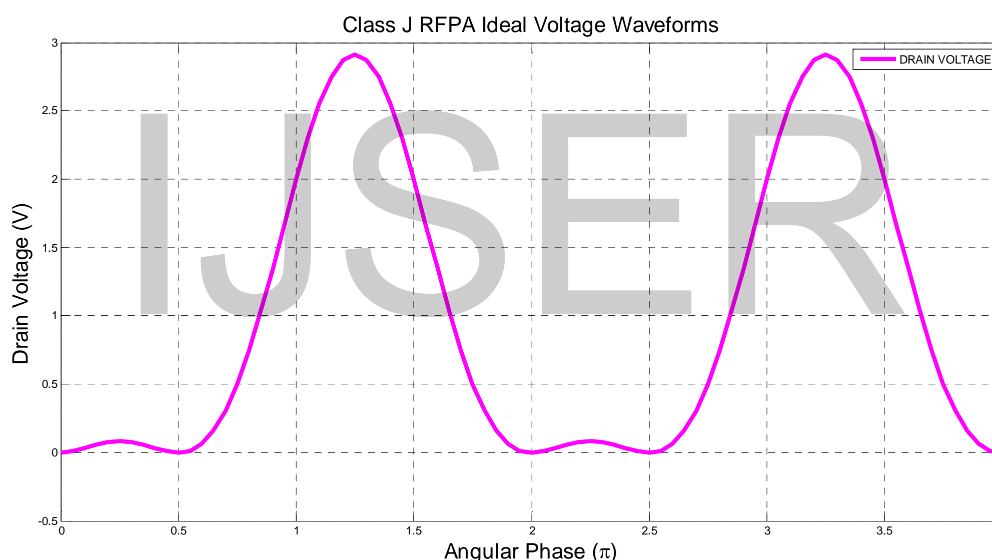

Figure 3.5: Class J RFPA Ideal Voltage Waveforms

As expressed in 3.17, neutralizing V_{dc}, we can also see that the Class J voltage contain only three contains: V_{dc}, fundamental and second harmonic voltages, thus resulting into:

$$V_{dc} = 1$$

$$V_{Fundamental}(\theta) = \sqrt{2}\sin(\theta + \pi + \frac{\pi}{4})$$

$$V_{2^{th}\ harmonic}(\theta) = -\frac{1}{2}\cos(2\theta + \pi - \frac{\pi}{2})$$

- 33 -

But considering that the drain current and voltage have an in-phase relationship, there is no DC component flows into the load. As such the Class J output parameters has only two components, therefore we obtained the final expressions for the output current and voltage entering into the load as indicated in equations (3.18) & (3.19).

$$I_{OUT} = \frac{I_{peak}}{2}\sin\theta - \frac{2I_{peak}}{3\pi}\cos 2\theta \quad (3.18)$$

$$V_{OUT} = \sqrt{2}\,V_{dc}\sin(\theta + \frac{\pi}{4}) - \frac{1}{2}V_{dc}\cos(2\theta - \frac{\pi}{2}) \quad (3.19)$$

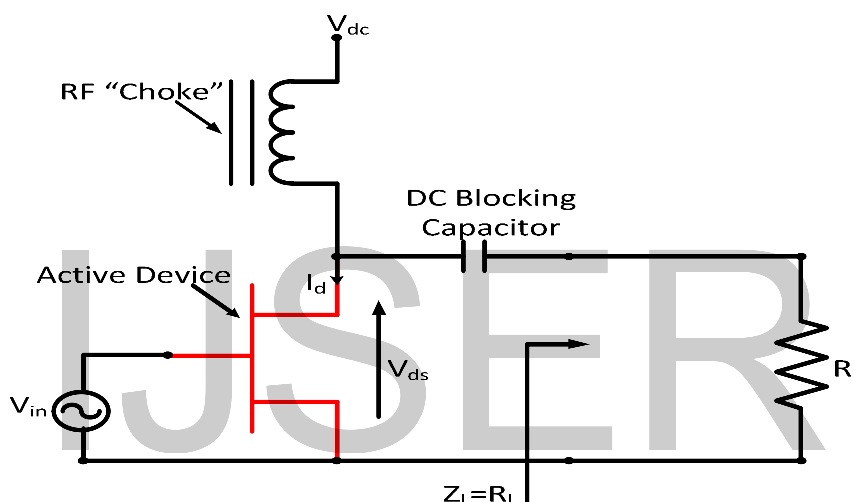

Figure 3.6: Intrinsic reverse phase relationship between drain current and voltage

Since that we have full details about the drain voltage and current of the Class J during it operational period, let's probe into others parameters essential to the discussion of RF power amplifiers. We begin with the calculation of the power output and the drain efficiency as expressed in the following equations:

$$P_{dc} = I_{dc}V_{dc} = \frac{I_{peak}}{\pi}V_{dc} \quad (3.20)$$

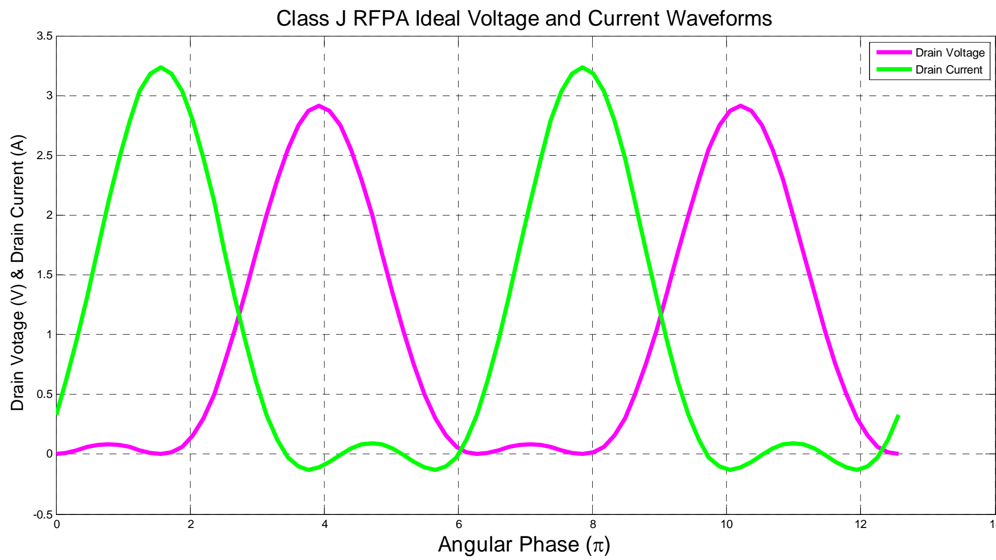

Figure 3.7: Class J RFPA ideal drain voltage and current waveforms over lapping @ lower amplitudes indicating lower power dissipated (P_D) at the output and reversed phase shift. See appendix C for Matlab codes that generate this plot

IJSER

Next, the power output can be calculated as earlier mentioned and seen below:

$$P_{OUT} = \frac{1}{2} Re\{V_{fundamental_OUT} I^{*}_{fundamental_OUT}\} \tag{3.21}$$

$$= \frac{1}{2} Re\left[\sqrt{2}V_{dc} \times e^{j\omega\frac{\pi}{4}} \times \frac{I_{peak}}{2}\right] = \frac{\sqrt{2}V_{dc}I_{peak}}{4} \cos\frac{\pi}{4}$$

Therefore the drain efficiency can be calculated as follows:

$$\eta_{drain} = \frac{P_{OUT}}{P_{dc}} = \frac{\frac{\sqrt{2}V_{dc}I_{peak}}{4}\cos\frac{\pi}{4}}{\frac{I_{peak}}{\pi}V_{dc}} = \frac{\pi}{4} = 78.54\% \tag{3.22}$$

The Class J RFPA theoretically has exactly the maximum drain efficiency as the Class B RF power amplifier. Additionally, under similar look, we can compute the Class J RF power amplifier load impedances at both the fundamental and second harmonic, given the same output current and output voltage as computed earlier. Also, still bear in mind that the phase shift of π in the equations are due to the shape of the waveforms as plotted in figure 3.7 and that of the nature of the Class J schematic as indicated in figure 3.6.

- 35 -

$$Z_{Lfundamental} = \frac{V_{Djfundamental}}{I_{Djfundamental}} = \frac{\sqrt{2}\,V_{dc}\angle\frac{\pi}{4}}{\frac{I_{peak}}{2}\angle 0} = \frac{2\sqrt{2}V_{dc}}{I_{peak}}\angle\frac{\pi}{4} \quad (3.23)$$

$$Z_{L2^{nd}harmonic} = \frac{V_{Dj2^{nd}harmonic}}{I_{Dj2^{nd}harmonic}} = \frac{-\frac{1}{2}V_{dc}\angle-\frac{\pi}{2}}{-\frac{2I_{peak}}{3\pi}\angle 0} = -\frac{3\pi}{4}\frac{V_{dc}}{I_{peak}}\angle(-\frac{\pi}{2}) \quad (3.24)$$

From equations 3.23 and 3.24, the Class J RFPA standard equations for the optimum load impedance at both fundament and second harmonic can be expressed as follow:

$$Z_{Lfundamental_opt} = \frac{2V_{dc}}{I_{Peak}} + j\frac{2V_{dc}}{I_{peak}} = R_{L_opt} + jR_{L_opt} \quad (3.23')$$

$$Z_{L2^{nd}harmonic_opt} = -j\frac{3\pi V_{dc}}{4I_{peak}} = -j\frac{3\pi}{8}R_{L_opt} \quad (3.24')$$

Also, we can achieve the fundamental and second harmonic load impedances by taking Fourier Transformation of the ratio of the fundamental and second harmonics voltage and current of the respective cases; this formulation is illustrated below:

IJSER

$$Z_{Lfundamental} = \frac{V_{Djfundamental}}{I_{Djfundamental}} = \frac{\sqrt{2}\,V_{dc}\sin(\theta+\frac{\pi}{4})}{\frac{I_{peak}}{2}\sin\theta} \quad (3.25)$$

$$Z_{L2^{nd}harmonic} = \frac{V_{Dj2^{nd}harmonic}}{I_{Dj2^{nd}harmonic}} = \frac{\frac{1}{2}V_{dc}\cos\left(2\theta-\frac{\pi}{2}\right)}{\frac{2I_{peak}}{3\pi}\cos 2\theta} \quad (3.26)$$

Simplifying equations (3.25) & (3.26) by applying addition & subtraction and the double angles of trigonometry function yield respectively equations (3.27) and (3.28).

$$Z_{Lfundamental} = \frac{2\sqrt{2}\,V_{dc}\cos(\theta)}{I_{peak}\sin\theta} \quad (3.27)$$

$$Z_{L2^{nd}harmonic} = \frac{3\pi V_{dc}\sin 2\theta}{4I_{peak}\cos 2\theta} = \frac{3\pi V_{dc}\sin\theta\cos\theta}{4I_{peak}(\cos\theta)^2 - 2I_{peak}} \quad (3.28)$$

Considering that $\theta = \omega_0 t$; where ω_0 *and* t is the center frequency and operational time of the signal respectively. Taking the Fourier transform of (3.27) & (3.28) give:

$$Z_{Lfundamental} = -\frac{j2\sqrt{2}V_{dc}[\delta(\omega+\omega_0)+\delta(\omega-\omega_0)]}{I_{peak}[\delta(\omega+\omega_0)-\delta(\omega-\omega_0)]} \quad (3.29)$$

$$Z_{L2^{nd}harmonic} = \frac{j3\pi^3 V_{dc}[\delta(\omega+\omega_0)-\delta(\omega-\omega_0)][\delta(\omega+\omega_0)+\delta(\omega-\omega_0)]}{4\pi^2 I_{peak}[\delta(\omega+\omega_0)+\delta(\omega-\omega_0)]^2-2I_{peak}} \quad (3.30)$$

Assuming that $4\pi^2 I_{peak}[\delta(\omega+\omega_0)+\delta(\omega-\omega_0)]^2 \gg I_{peak}$, equation (3.30) reduces to equation (3.31) as seen below:

$$Z_{L2^{nd}harmonic} = \frac{j3\pi V_{dc}[\delta(\omega+\omega_0)-\delta(\omega-\omega_0)]}{4I_{peak}[\delta(\omega+\omega_0)+\delta(\omega-\omega_0)]}$$

IJSER

Similarly as done before, we can select values for $V_{dc}, I_{peak}, \omega_0$ *and* ω to get some working values for the fundamental and second harmonic impedances.

The Class J RFPA in relation to the Class B lower power dissipation at the output can also be seen in figure 3.8 (a & b), which indicates the harmonic components of the output power for both Class B & J respectively. As shown in the plots, the class J has less DC power dissipation (≈ 0.1W) at its output, whereas, the Class B showed higher DC power dissipation (≈0.4W) at its output. Thus, the Class J RFPA has less output power given the same efficiency as with that of Class B RFPA.

- 37 -

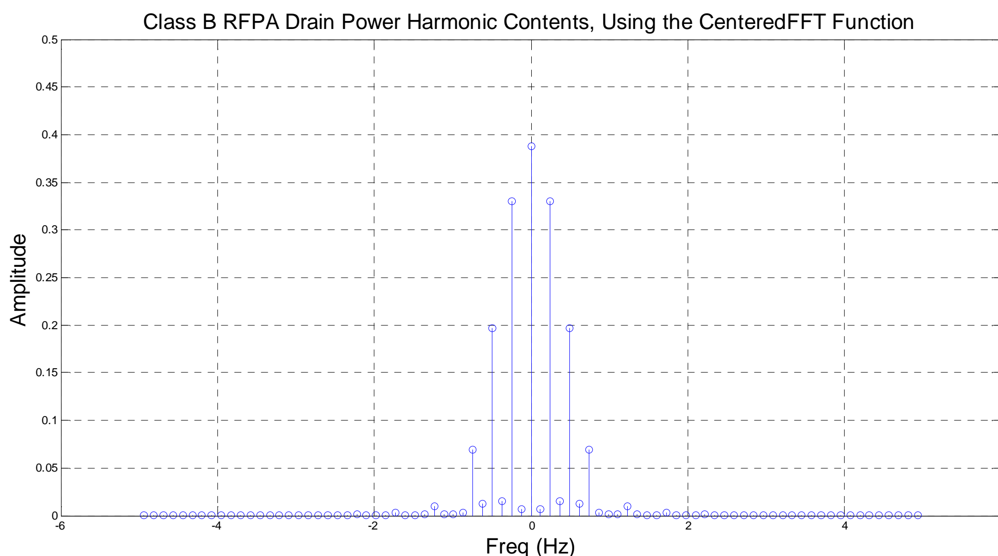

Figure 3.8a

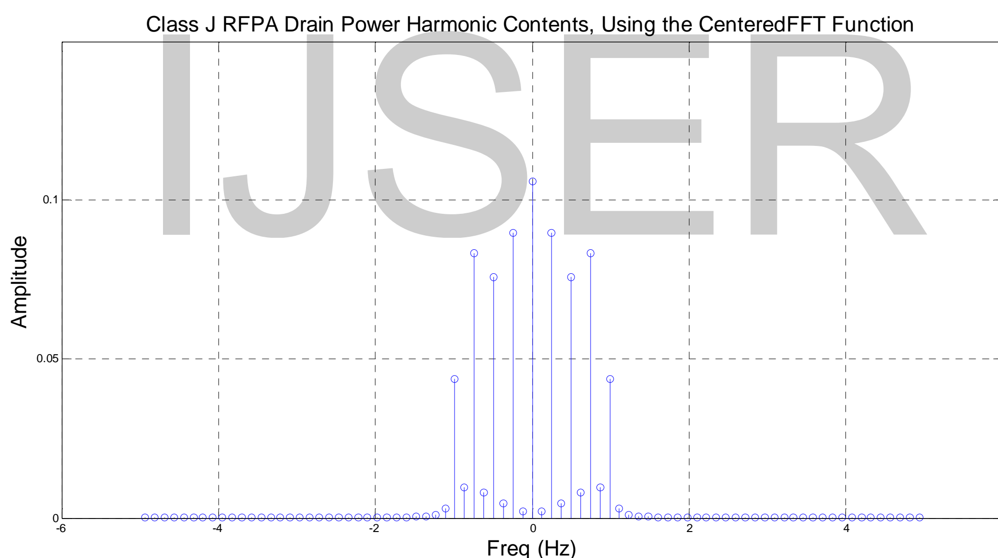

IJSER

Figure 3.8b

Figure 3.8 (a & b): Amplitude of Class B & J RFPA output Powers, (a) & (b) respectively

3.3 Class J Essential

Chapter two and this chapter have proven that the Class J have similar performance characteristics in comparison to the wide adopted Class B; but what arises to one mind is the question, "why Class J RFPA"? In providing some clues to this question, let's consider the frequency performance of both the

- 38 -

Class B and Class J in keeping with their loads position(s) on the Smith Chart. Seen in figure 4.21, is the load impedance of the Class B RFPA which showed purely resistive at the fundamental and shorted load (Z_{2nd} =0); this condition causes the class B RFPA to be limited in frequency band: in fact it is not possible, in presence of parasitics, to ensure a constant load termination at the variation of frequency. As such the Class B RFPA being a high efficiency power amplifier, the manipulation of it for wideband performance lead to the formation of the emerging Class J RFPA.

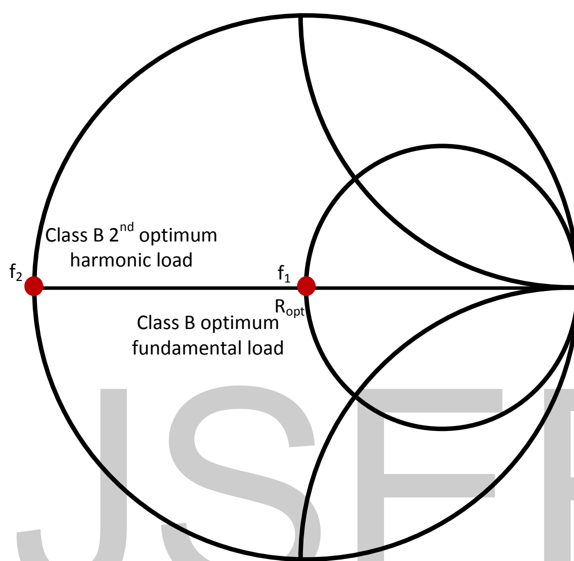

IJSER

Figure 4.21: Smith Chart indicating Class B fundamental and 2nd harmonic load position, which limits wideband capability to narrow band

Contrary to the loads condition on the Smith Chart, the Class J load plotted showed resistive and reactive at the fundamental $(Z_{Lfundamental_opt} = R_{L_opt} + jR_{L_opt})$ and purely negative reactive load at the second harmonic $(Z_{L2^{nd}harmonic_opt} = -j\frac{3\pi}{8}R_{L_{opt}})$. Such load condition, that is different from the one of the class B, enable the family of class B and class J RFPA to possess wideband capability. As indicated in figure 4.xxx, frequency swing can take place between the real load and positive reactive load of the fundamental, that is from $f_1\ to\ f_2$ as indicated with the red line and similarly for the second harmonic load, the frequency swing take place between the shorted load points from $2f_1 to\ 2f_2$, this illustration is shown in figure

4.22. Thus leading the Class J to function in the wideband range; owing on these clues the following are pointed out for the Class J importance:

- We want to prove that class J performance operation described in this research shows similar output power and drain efficiency to be obtained in comparison to the widely used Class B.

- The combination of class B and J can be useful to extend the bandwidth, in fact the same performances in terms of power and efficiency are achieved, but in different load conditions.

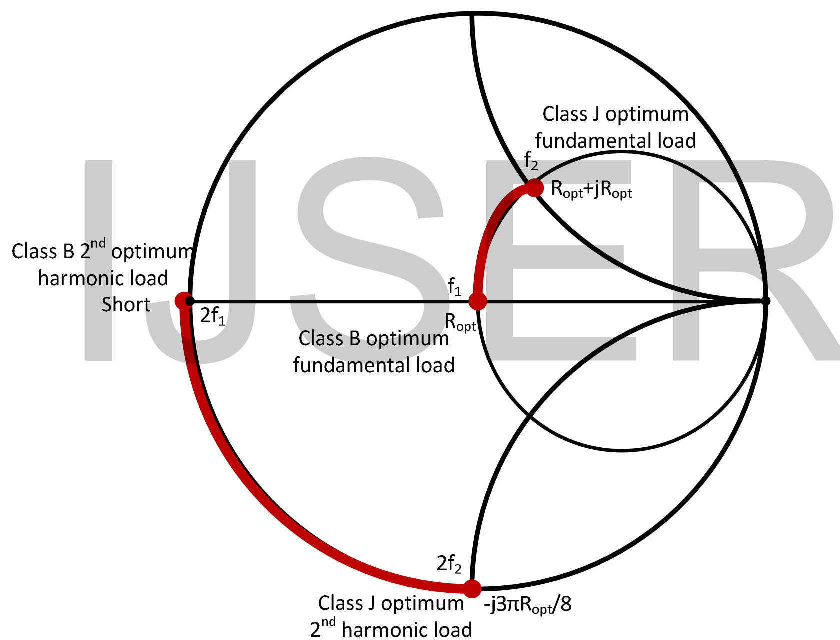

Figure 4.22: Smith Chart indicating Class J fundamental and 2nd harmonic load position, which impact its wideband capability

Chapter Four

4.0 Simulations and theoretical comparisons

In this chapter, simulation results of various performances yield from Class A, B and J RFPA have been obtained using large signal models of a GaN HEMT. The adopted transistor has a non-linear model delivered by the seller, but as first approach, a simplified– ideal model is adopted, with DC characteristic similar to the real device. These results have been evaluated in line with those from the theoretical analysis indicated in Chapters two and three. In particular, comparison is led observing the drain voltage and current waveforms, input power, output power and drain efficiency. Then, the simulations are carried with the real non-linear model of the device, focusing on the emerging difficulties and degraded performances in the design, due mainly to the presence of parasitic elements.

4.1 Simulations

4.1.1 IV and Transcharacteristics Curves

The first step is the simulation of the output characteristics of the large signal model of the GaN HEMT by Nitronex (NPTB00004 device), the transistors model intended to be used for the actual design of the Class J. We adopted the Santaklaus model as simplified nonlinear model, which is an ideal mathematical model that entails some iteration processes, that's varying the coefficients $a_0, a_1, a_2, and\ a_3$ and selecting suitable value of the amplifier breakdown voltage (V_{brd}), saturation drain current (I_{dss}), knee voltage (V_{knee}) and pinch-off voltage (V_{po}) based on need of the device model to be designed. Here, a0…a3 are the coefficients of the polynomial of the gate IV characteristics of the device to be designed: in this case, we tried to fit the real device characteristic we considered only a0, a1. As seen in the schematics, 400mA, -3V, 100V, 4V, 1.41 and 0.81 were obtained for $I_{dss}, V_{po}, V_{brd}, V_{knee}, a_0\ and\ a_1$ respectively; only $a_0\ and\ a_1$ were considered because up to the second harmonic of the output signal of the device being designed is considered. Thus these results of the Santaklaus yield similar IV characteristic as those of the NPTB00004 device to be used for the actual design, taking into account the IV characteristics curves of the both devices as depicted in figure 4(a & b). In keeping with these results, we were at the conviction that this

IJSER

- 41 -

configuration of the Santaklaus model serves as a suitable model for the Nitronex device, so those parameter gathered were used to implement the design using the NPTB00004 device.

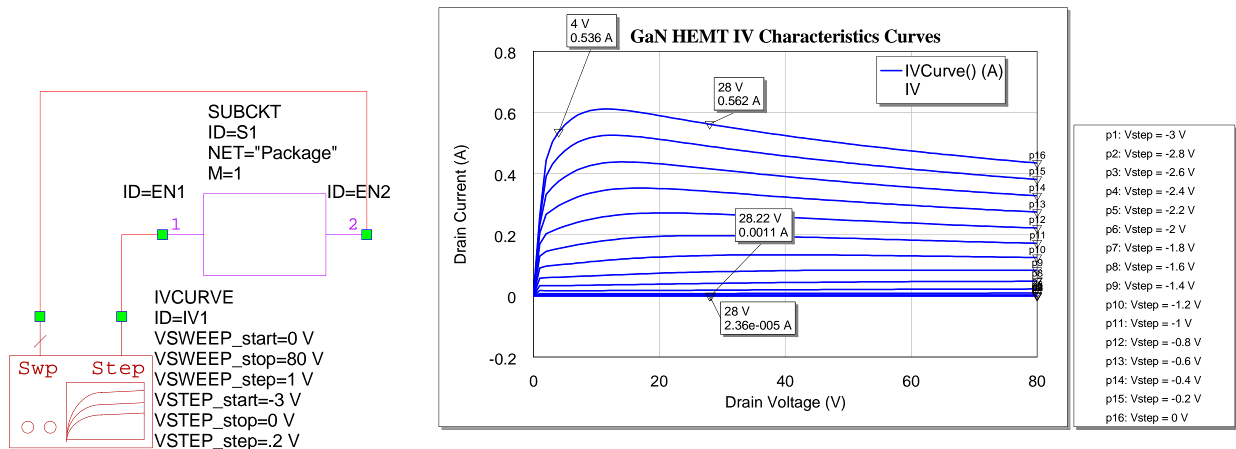

Figure 4.1(a): GaN HEMT IV Characteristics

IJSER

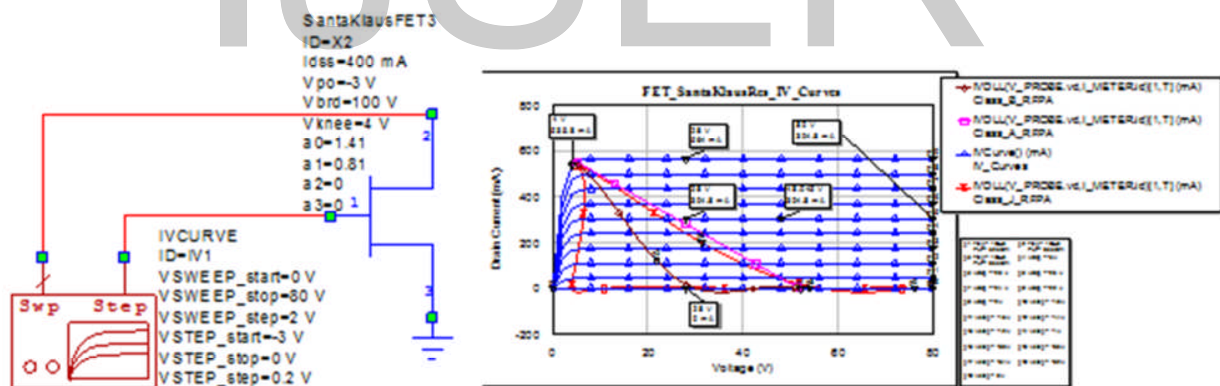

Figure 4.1(b): SantaklauRES drain current and drain voltage characteristics curves

Also, in order to obtain the various biasing points of the amplifier classes, the transcharacteristics curves for both models were generated; from this curve, a V_{GS} of 0.87V was extracted for the class A and of -1.8V was extracted for both Class B & J; figure 4.2 shows these curves.

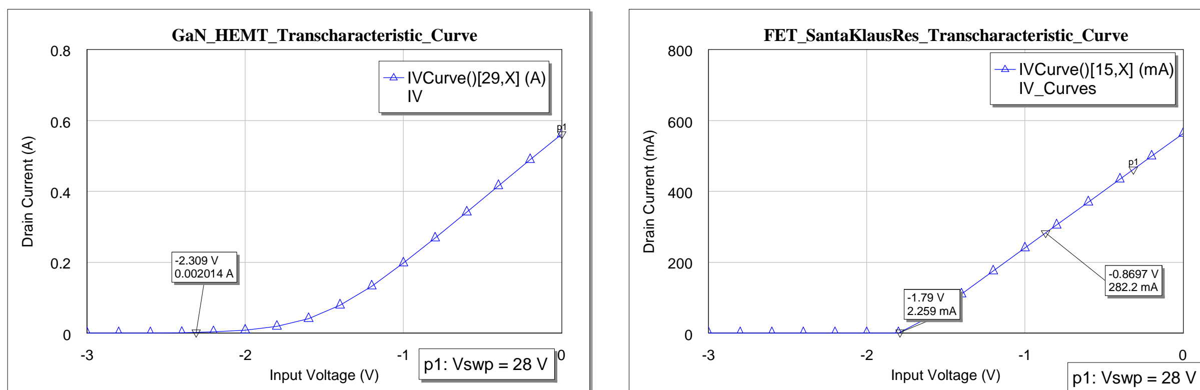

Figure 4.2: The GaN HEMT and SantaklausRes Models transcharacteristics curves, indicating the pinch-off of the models. The pinch-out of the GaN HEMT model was used for model because it's the model to be used for the actual design.

4.1.2 Schematics, Drain Voltage and Current Generation

Aim at achieving the similar drain voltage and drain current waveforms of the RFPA Classes (B and J) as those obtained with the theoretical analysis, ideal components were used to achieve these goals; these are illustrated in the respective schematics of the RFPA classes below. Basically, these components are Biastee and resonators; the biastee contains a capacitor which block the DC input from entering into the RF input and an inductor which is responsible for stopping the RF components from entering the DC port. The biastee at the gate input combined both RF and DC signal transmit to the gate while the one at the drain port allows only the RF component be passed to the load. The resonator used in this modeling is a general resonator that is contained in the Santaklaus library: it is an ideal mathematical resonator which can be used in several resonating conditions. As such it can be configured to be used as the normal resonator as it has been applied in this design work. In some cases, it was configured to allow specified signal spectral components to pass through, that is short at a given frequency, and in other cases it was modeled to block other specified components from entering, that is open for a given frequency components; thus it has an arbitrary behavior in operation.

IJSER

- 43 -

4.1.2.1 Class A

The schematic of an ideal Class A RFPA is exemplified in figure 4.3. In this figure, there is no resonator needed in the circuit because there is no need to block any of the generated signal components from entering the load (being the SantaKlaus an ideal model, there is no harmonic generation in Class A, at least up to compression). Drain voltage and drain current for this network is shown is figure 4.4; these results are similar to those of figure 2.5(A) in chapter two.

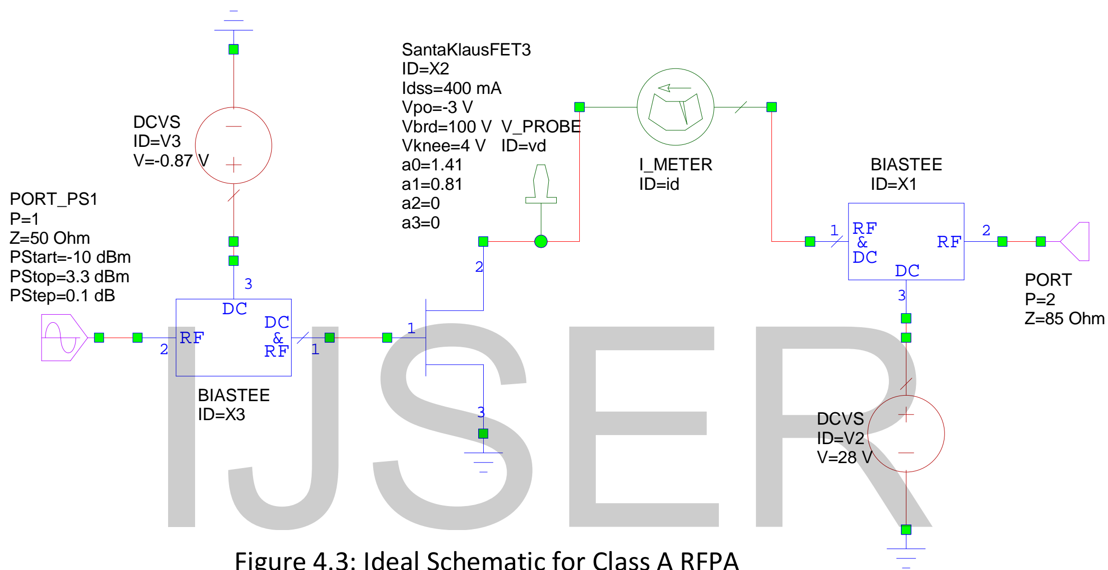

Figure 4.3: Ideal Schematic for Class A RFPA

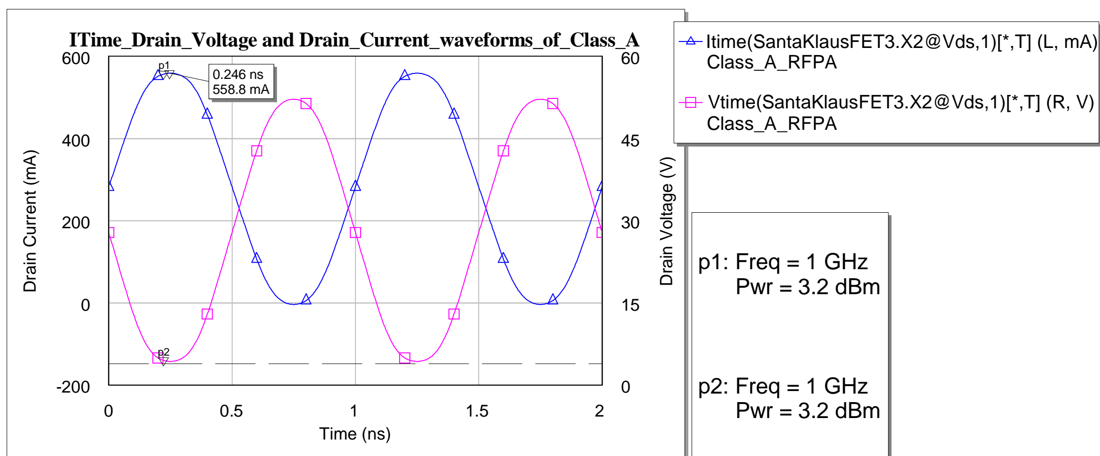

Figure 4.4: Ideal Class A RFPA drain voltage and Drain current waveforms

IJSER

- 44 -

4.1.2.2 Class B

Contrary to the Class A, the Class B RFPA schematic showed a resonator circuit which allow only the fundament component to enter the load and terminates all other harmonics from entering the load (in particular, we refer here to the Tuned Load Class B); figure 4.5 shows this formulation.

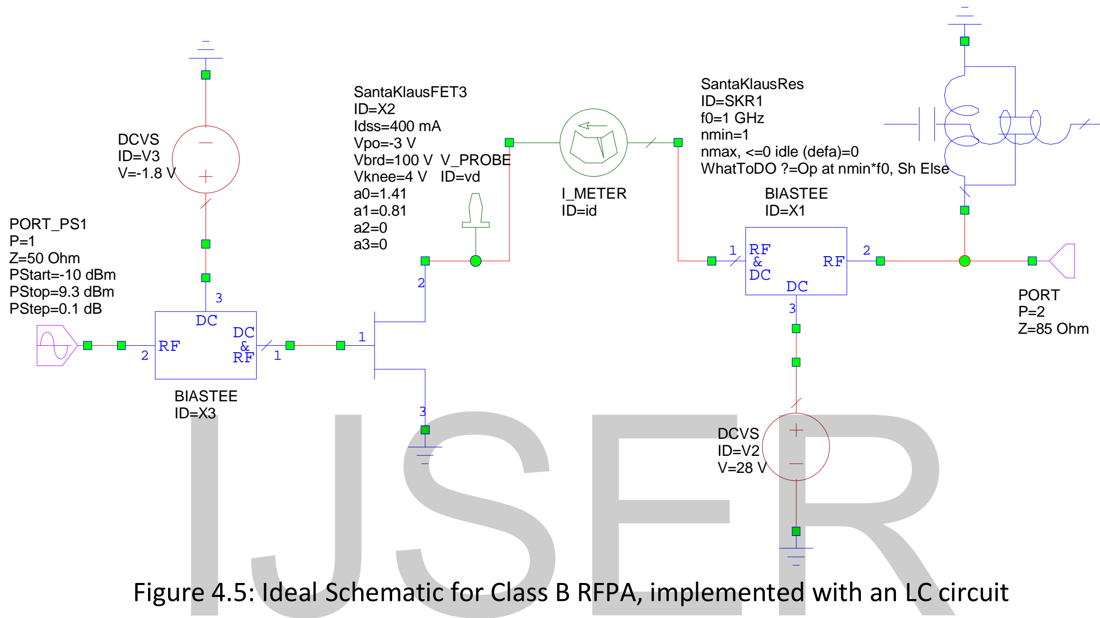

IJSER

Figure 4.5: Ideal Schematic for Class B RFPA, implemented with an LC circuit

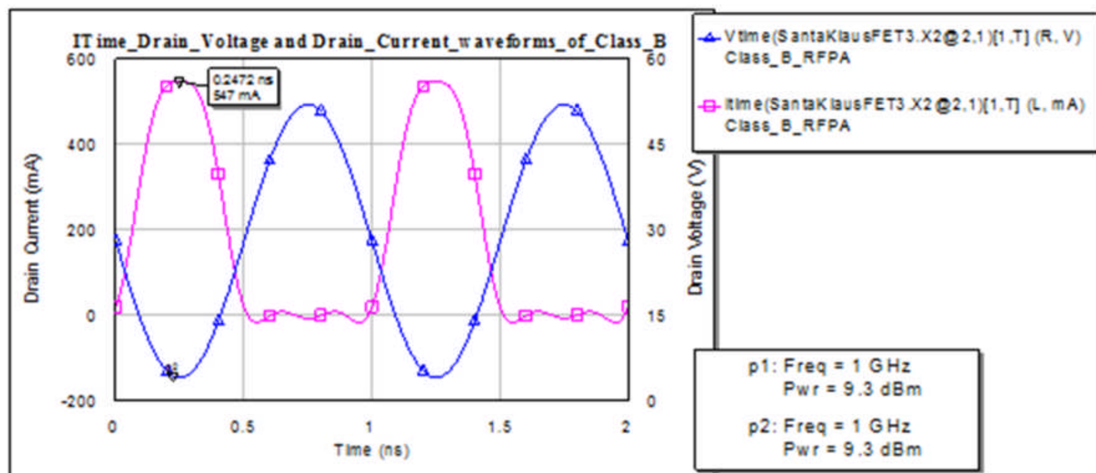

Figure 4.6: Ideal Class B RFPA drain voltage and Drain current wavefoms

From the network indicated in figure 4.5, the drain voltage and drain current waveforms were achieved; these waveforms are shown in figure 4.6. As seen in the figure, the waveforms generated are similar to those generated using Matlab in chapter two.

4.1.2.3 Class J

The Class J network is similar to that of the Class B, but the Class J has two additional parallel resonators and its optimum load is a complex impedance, that can be implemented, at least in a preliminary analysis, as a series inductor- resistor. As seen in the schematic, figure 4.7, there are three resonance circuits, the first, SKR1 is configured such that only the fundamental component enters the load, and the fundamental termination does not affect the other harmonics. The second, SKR2 is responsible for blocking the fundamental component and allows all other harmonic to pass through. As seen in the network, the capacitor, CAP is the second harmonic load impedance as earlier derived, but this CAP required only the second harmonic so the third resonator, SKR3 is required to block the second harmonics to be received by CAP and all other harmonics beyond the second to pass through. Therefore, it is clearly implemented that the Class J is terminated at the second harmonic. Given such nature of the network, we are able to obtain half sine wave similar that of the Class B for the drain current and quasi sine wave for the drain voltage these waveforms are illustrated in figure 4.8; the

IJSER

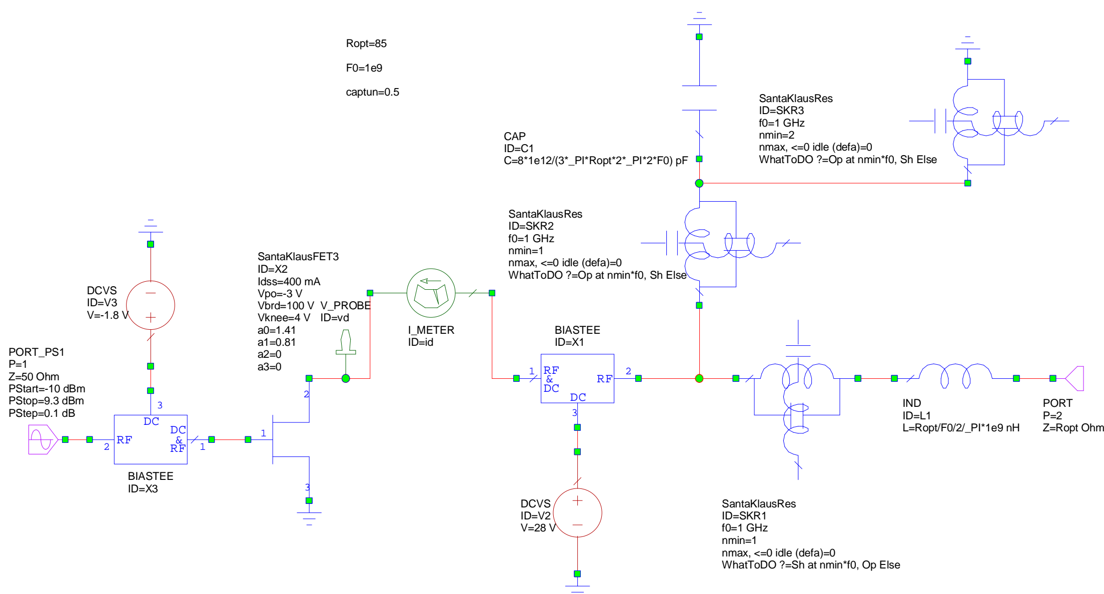

Figure 4.7: Ideal Schematic for Class B RFPA, implemented with an LC circuit

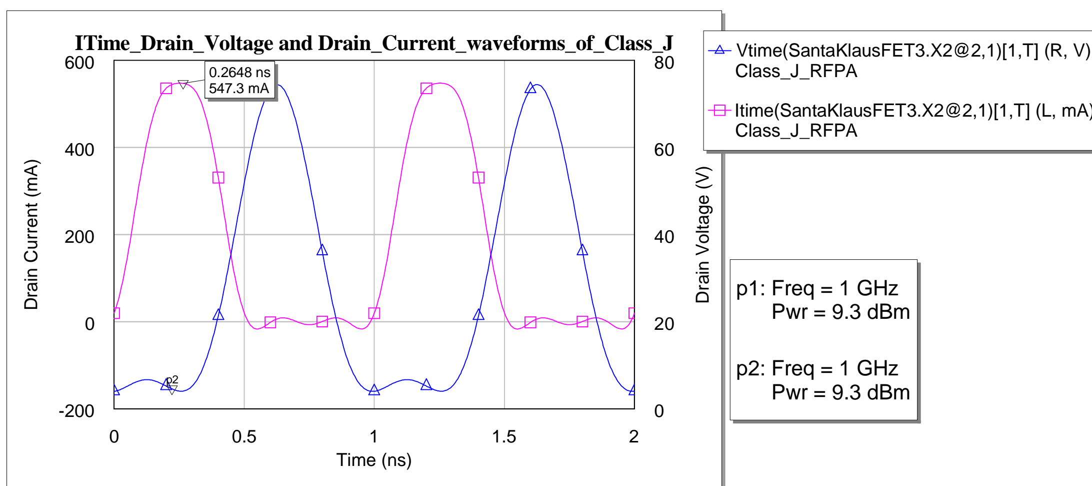

Figure 4.8: Ideal Class J RFPA drain voltage and Drain current waveforms

4.2 Output Power and drain efficiency Comparisons

In this section, the theoretical parameters, such as output power and drain efficiency are being compared to the ones achieved using the MWO software considering the same input power. As indicated in the previous chapters, the maximum theoretical efficiency for Class A and B & J are 50% and 78.54% respectively. The Class A in the simulation showed performance little below this maximum efficiency which may be at the result of the proper biasing condition and knee voltage. Similarly, the Class B & J showed lower value (about 68.24%) as compare that of the theoretical one; this is due to the effect of the knee-voltage. These results are shown in the below figures. Figure 4.9 shows comparison between Class A and Class B; as exemplified by this figure, Class B showed higher efficiency as compare to Class A RFPA and lower gain (6 dB penalty) output power to that of class A as expected from theory.

IJSER

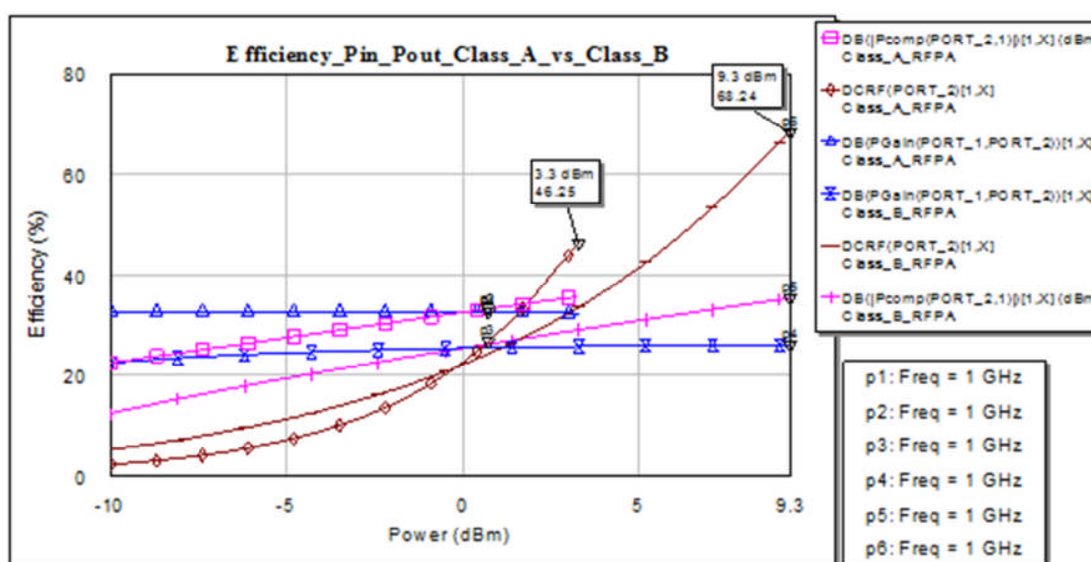

Figure 4.9: Comparison between Class A RFPA and Class B RFPA, efficiency, input and output power

Additionally, figure 4.10 illustrates comparison between Class B and Class J, one of the interests of concern for this work, as showed in the figure, both amplifiers proved being equal in the various parameters, input and output power and efficiency at every interval. Again, we can attribute these reductions in efficiencies due to some harmonic components still interplaying with the fundamental component in both devices.

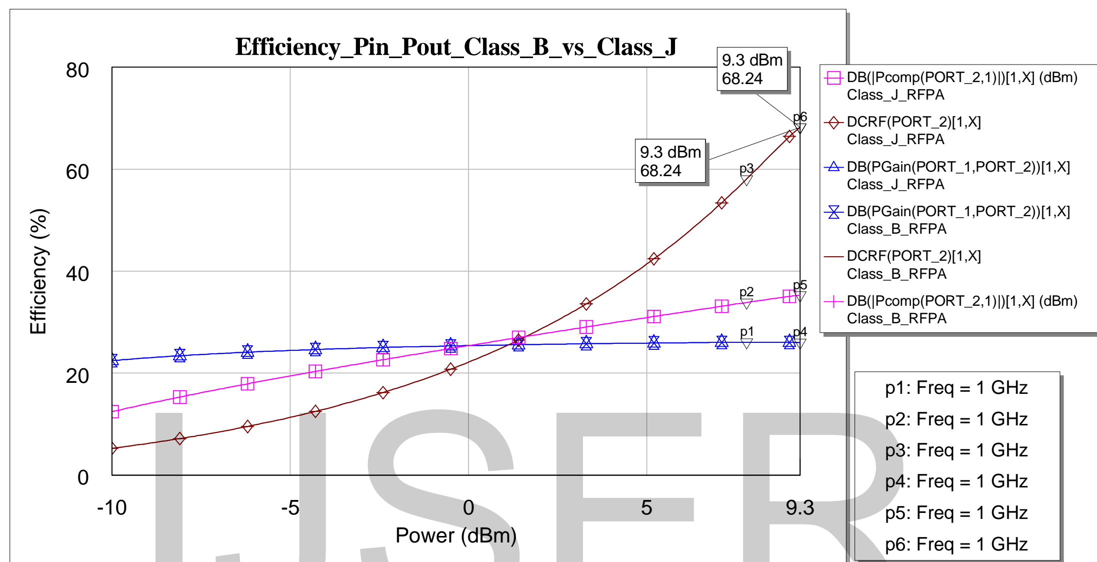

IJSER

Figure 4.10: Comparison between Class B RFPA and Class J RFPA, efficiency, input and output power

4.3 Design with lumped element Resonators

Aims at leaving from the complete ideal design, that is using the Santakluas Resonators, the following were considered in response to the output network matching of both Class B and J RFPA.

4.3.1 Class B

As depicted in figure 4.11 resonance circuits embedded in MWO were used considering the design frequency (1GHz) of this project. Serious iterations were carried out to obtain suitable values for the capacitors and inductors that makeup the resonator circuit. These iterations results are tabulated in table 4.1; from these values, it is reasonable to indicate which particular values of capacitors and inductors (chosen in a reasonable range) are need for better performances in terms of output power, efficiency.

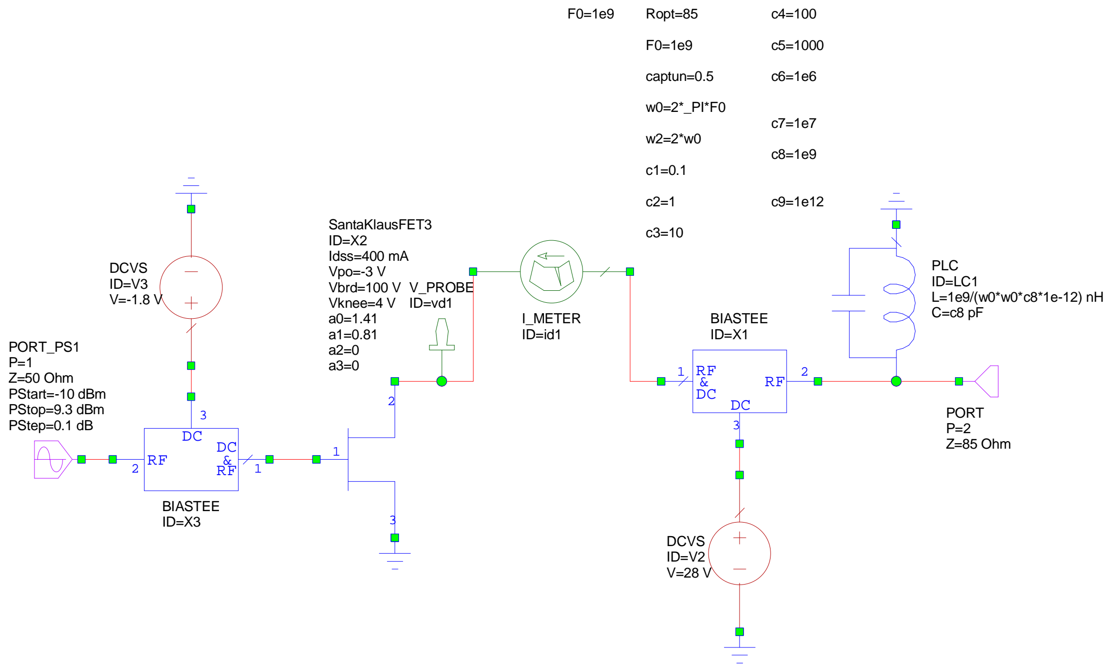

Figure 4.11: Class B network without Santakluas Resonator

IJSER

As listed in table 4.1, certain ranges of capacitors and inductors are more preferable, thus from the iterations performed capacitors C_1, C_2, C_3 *and* C_4 and their corresponding inductors L_1, L_2, L_3 *and* L_4 (mainly C_3 & L_3 *and* C_4 & L_4) are recommended for better device choice in view of the better device choice mentioned earlier.

Table 4.1: Some preferable value for figure 4.11 optimum design performance

CAP (pF)		IND (nH)		η (%)	P_{OUT} (dBm)	I_{MAX} (mA)
C_1	0.1	L_1	253.3	60.22	34.36	568.9
C_2	1	L_2	25.33	61.85	34.58	486.5
C_3	10	L_3	2.53	68.04	35.27	544.7
C_4	100	L_4	0.253	68.24	35.29	547
C_5	1000	L_5	0.0253	68.24	35.29	547
C_6	10^6	L_6	$2.53x10^{-5}$	68.24	35.29	547
C_7	10^7	L_7	$2.53x10^{-6}$	68.24	35.29	547
C_8	10^9	L_8	$2.53x10^{-8}$	68.14	35.29	547
C_9	10^{12}	L_9	$2.53x10^{-11}$	$8.88x10^{-15}$	0	569.2

- 49 -

Also, gearing at providing evidence for the choice of the capacitors and inductors values selected from table 4.1, shown in figure 4.12 are plots of the drain voltage and drain current characteristic curves using C_3 and L_3 of figure 4.11.

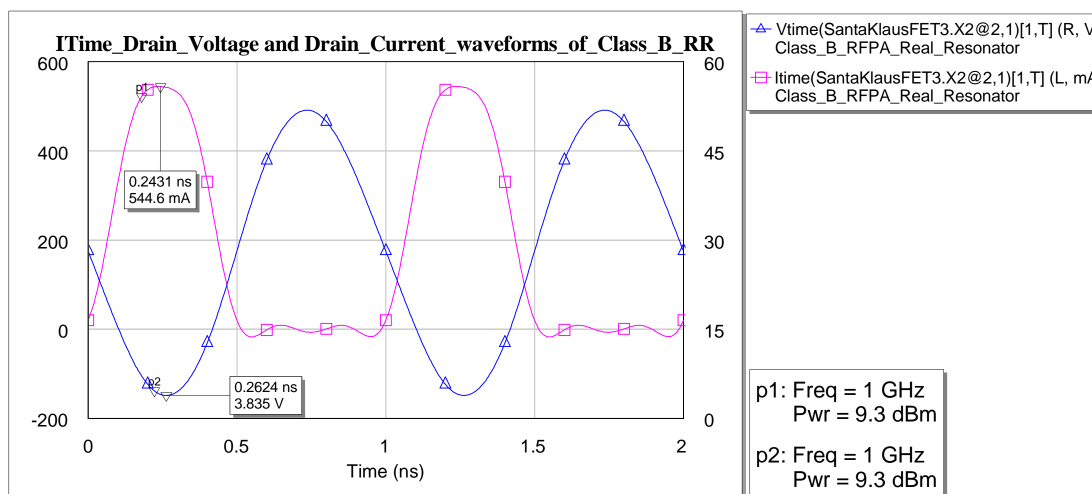

Figure 4.12: IV characteristics Class B network using real resonators
(Without Santakluas Resonator)

IJSER

4.3.2 Class J

Similarly as done in the case of Class B were done for class J as indicated in figure 4.12. Three resonators obtained from MWO were design to replace the santakluas resonators models. In the case of Class J, in order to obtain desirable values of the resonators circuits so as to achieve better performance of the device, each of the designed resonators was used along with either of the other two Santaklaus Resonators in order to check the response of the actual resonance circuit. With this process, table 4.2 (A & B) was generated in order to show selected capacitors and inductors values for the respective actual resonators network. Also for a better choice of device, the following family of capacitors and inductors are recommended for used as per the network structure of figure 4.13.

- 50 -

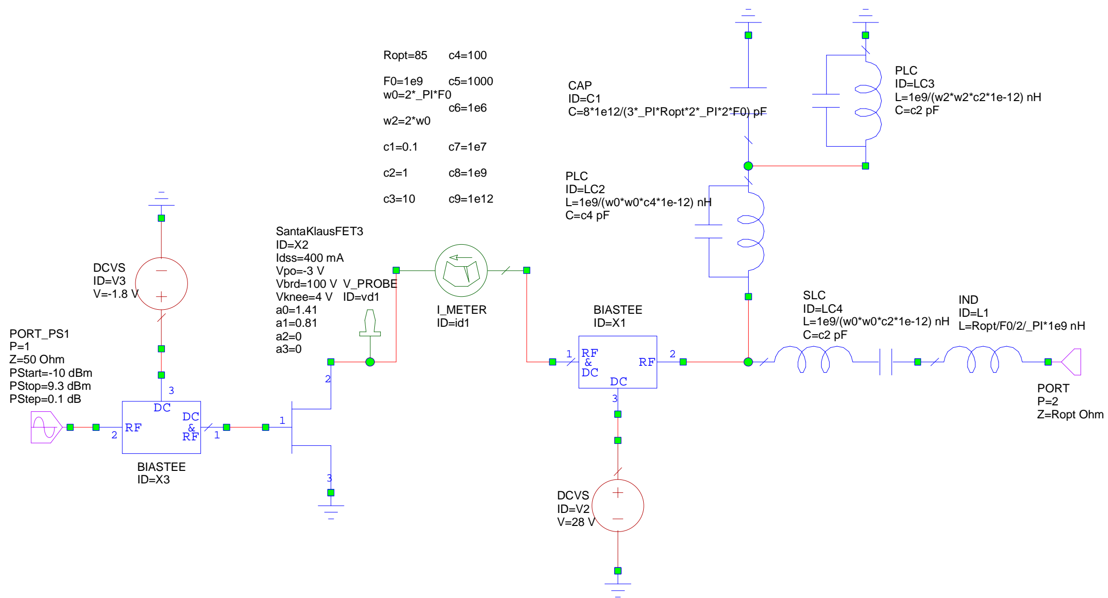

Figure 4.13: Class J network without Santakluas Resonator

IJSER

Table 4.2: Selected components values for implementing Class JRFPA using real resonators					
Table 4.2 (A): Family A					
Resonator SRC ID-LC4		Resonator PRC ID-LC2		Resonator PRC ID-LC3	
C (pF)	0.1	C (pF)	10	C (pF)	0.1
L (nH)		L (nH)		L (nH)	
η (%)	68.29				
I_{MAX}(mA)	549				
P_{OUT} (dBm)	35.27				

Table 4.2 (A): Family B					
Resonator SRC ID-LC4		Resonator PRC ID-LC2		Resonator PRC ID-LC3	
C (pF)	1	C (pF)	100	C (pF)	1
L (nH)		L (nH)		L (nH)	
η (%)	66.81				
I_{MAX}(mA)	526.2				
P_{OUT} (dBm)	35.27				

Plotted in figure 4.14 are the plot for the IV characteristic figure 4.13 displaying similar drain voltage and drain current waveforms as plotted in previous cases for the Class J RFPA and also indicating accurate selection of the device components. From the plots, it is observable that the condition set for I_{dss}, V_{brd} and V_{knee} are met and the family A components were selected for these plots.

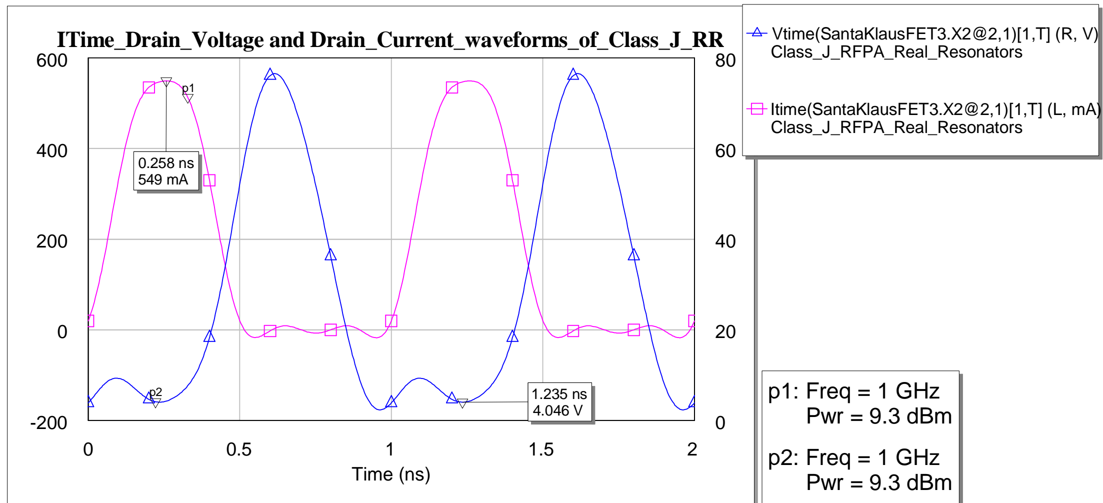

Figure 4.14: IV characteristics Class J network using real resonators (Without Santakluas Resonator)

IJSER

4.3.3 Output and drain efficiency Comparisons (without Santakluas resonators)

Subsequently, figure 4.15 illustrate the plots of the drain efficiency, input and output powers for both Class B and Class J RFPA. Certainly, as exemplified by figure 4.15, the choice of the component values

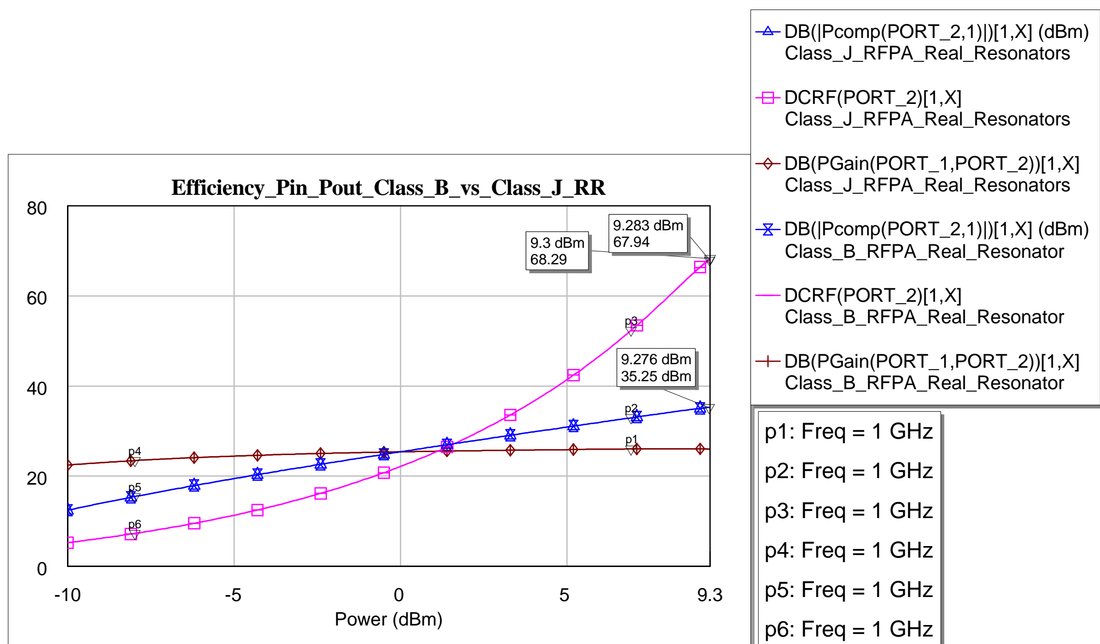

Figure 4.15: Drain efficiency, input and output power of both Class B and Class J using actual resonators.

were wisely selected thus yielding similar efficiency and output power for the both devices which is still keeping us on track with the theoretical meaning of the devices; that is class B and J have about the same drain efficiency and output power given the same input power.

4.4 Class B Design – with lumped element biastee

Still considering removing all ideal components for the device, the Class B can be implemented using the below network as illustrated in figure 4.16. In this network, the biastee is implemented using the resonator circuit and the drain is feed between the resonator and a bypass capacitor (c_1). This bypass capacitor filters the RF components going into the DC supply and block the noise from the DC supply to the circuit.; and the resonator blocks all harmonics from entering the load, thus allowing only the fundamental to flow through the load. Lastly, as seen in the network is an output capacitor (C_2) that blocks the DC component entering the load. As such, the capacitances of the bypass capacitor and the output capacitor are very large with respective to the capacitance of the resonator circuit; again suitable choice of these capacitors should be exploited so as to achieve maximum performance of the device. Based on this, some iteration was performed in MWO to obtain values for all capacitors in the network that yield optimum performance of the device. As a result, table 4.3 shows ranges of capacitances and inductances that can be selected to give desire/optimum results.

IJSER

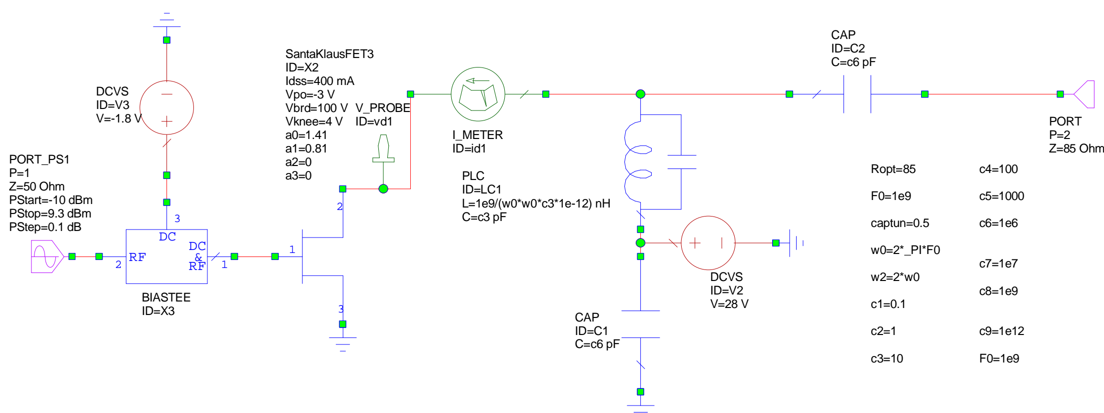

Figure 4.16: Class B RFPA implemented using Bypass capacitor and output capacitor (without a biastee)

Table 4.3: Selected components values for implementing Class BRFPA using real resonators, byepass capacitor and output capacitor					
Family A		Family B		Family C	
C1(pF)	10	C1(pF)	100	C1(pF)	1000
L1(nH)	2.533	L1(nH)	0.2533	L1(nH)	0.0253
C_{BPASS}(pF)	10^6	C_{BPASS}(pF)	10^6	C_{BPASS}(pF)	10^6
C_{OUT}(pF)	10^6	C_{OUT}(pF)	10^6	C_{OUT}(pF)	10^6
η (%)	68.04	η (%)	68.24	η (%)	68.24
P_{OUT} (dBm)	35.27	P_{OUT} (dBm)	35.29	P_{OUT} (dBm)	35.29
I_{MAX}(mA)	544.7	I_{MAX}(mA)	547	I_{MAX}(mA)	546.9
Family D		Family E		Family F	
C1(pF)	10^6	C1(pF)	1	C1(pF)	1
L1(nH)	$2.533x10^{-6}$	L1(nH)	25.33	L1(nH)	25.33
CBPASS(pF)	10^6	CBPASS(pF)	1000	C_{BPASS}(pF)	10^6
C_{OUT}(pF)	10^6	C_{OUT}(pF)	1000	C_{OUT}(pF)	10^6
η (%)	68.24	η (%)	61.85	η (%)	61.85
P_{OUT} (dBm)	35.29	P_{OUT} (dBm)	34.58	P_{OUT} (dBm)	34.58
I_{MAX}(mA)	547	I_{MAX}(mA)	486.6	I_{MAX}(mA)	486.4
Family G		Family H		Family I	
C1(pF)	1	C1(pF)	1	C1(pF)	0.1
L1(nH)	25.33	L1(nH)	25.33	L1(nH)	253.3
CBPASS(pF)	100	CBPASS(pF)	10	CBPASS(pF)	10^{12}
C_{OUT}(pF)	100	C_{OUT}(pF)	10	C_{OUT}(pF)	10^{12}
η (%)	61.82	η (%)	61.17	η (%)	60.22
P_{OUT} (dBm)	34.57	P_{OUT} (dBm)	34.49	P_{OUT} (dBm)	34.36
I_{MAX}(mA)	488.4	I_{MAX}(mA)	501.4	I_{MAX}(mA)	466.7
Family J		Family L		Family M	
C1(pF)	0.1	C1(pF)	0.1	C1(pF)	
L1(nH)	253.3	L1(nH)	253.3	L1(nH)	
C_{BPASS}(pF)	10^6	C_{BPASS}(pF)	10	CBPASS(pF)	
C_{OUT}(pF)	10^6	C_{OUT}(pF)	10	C_{OUT}(pF)	
η (%)	60.22	η (%)	60.02	η (%)	
P_{OUT} (dBm)	34.36	P_{OUT} (dBm)	34.33	P_{OUT} (dBm)	
I_{MAX}(mA)	466.7	I_{MAX}(mA)	475.8	I_{MAX}(mA)	

IJSER

- 54 -

Also, aim at providing evidence that reasonable values of the components that yield optimum performance have been selected, figure 4.17 shows the plots of the IV characteristic curves and figures 4.18 shows the plots of the drain efficiency, input power and output power. Again, as seen in figure 4.17, the definition of the Class B RFPA has been fulfilled once more, here the family B as indicated in table 4.3 was selected to achieve these plots.

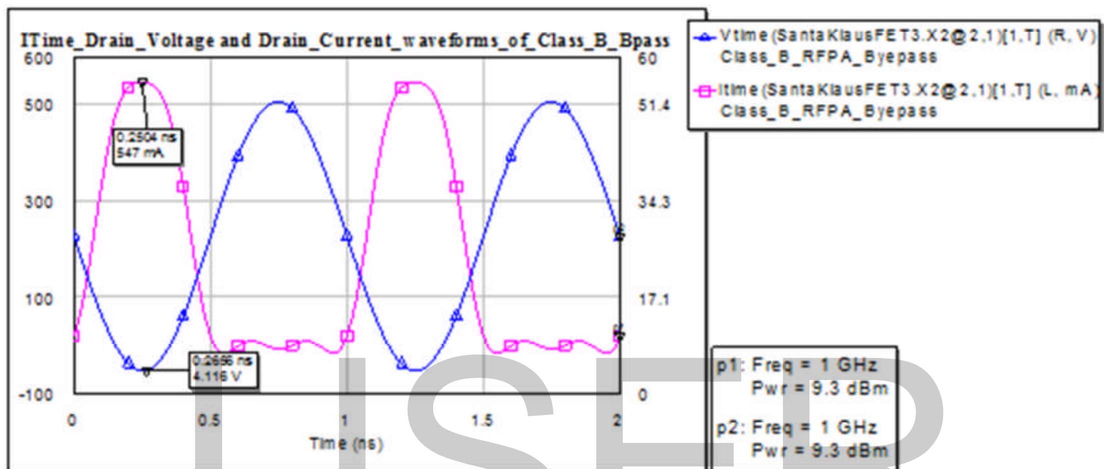

IJSER

Figure 4.17: I/V Characteristic curves of Class B RFPA implemented using Bypass capacitor and output capacitor (without a biastee)

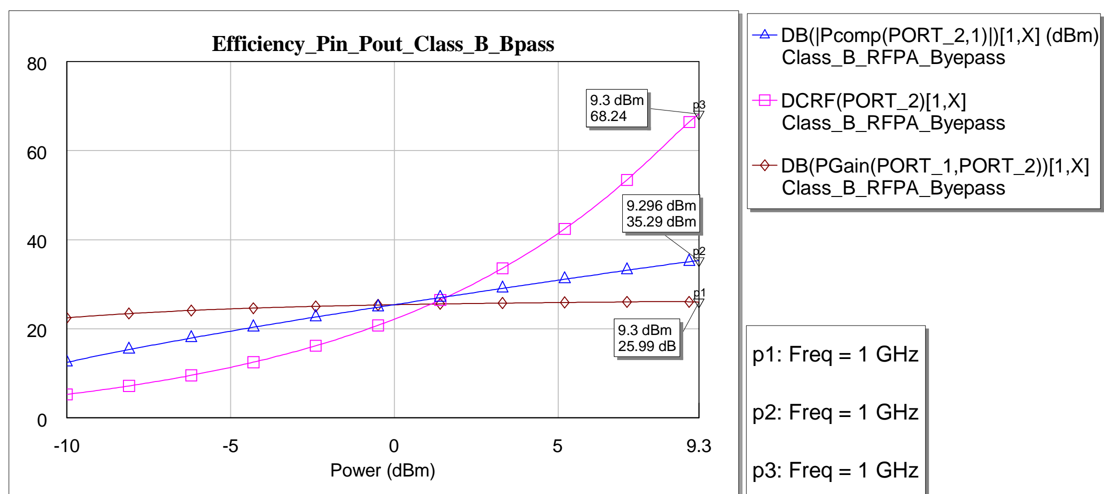

Figure 4.18: Drain efficiency, input and output power of Class B RFPA implemented using Bypass capacitor and output capacitor (without a biastee)

4.5 Parasitic element consideration – Class B.

Still on the basis of leaving completely the ideal design, now considered is the GaN HEMT parasitic, C_{DS} (1pF- obtained from device data sheet); in this vein we place a capacitor equivalent to C_{DS} in parallel to the drain of the device model. Considering this configuration, as illustrated in figure 4.19, the parasitic capacitor, C_{DS} of the transistor combined in parallel with the capacitor, C_{LC} of the resonance circuit, so the inductor, L_{LC} of the resonance circuit sees a capacitor equivalent to the sum of CDS and C_{LC} $(L_{LC} = C_{LC} + C_{DS})$. Given this situation, the output network is matched, thus yielding similar efficiency and output power as compare to the design done without considering the parasitic of the transistor in the case of Class B.

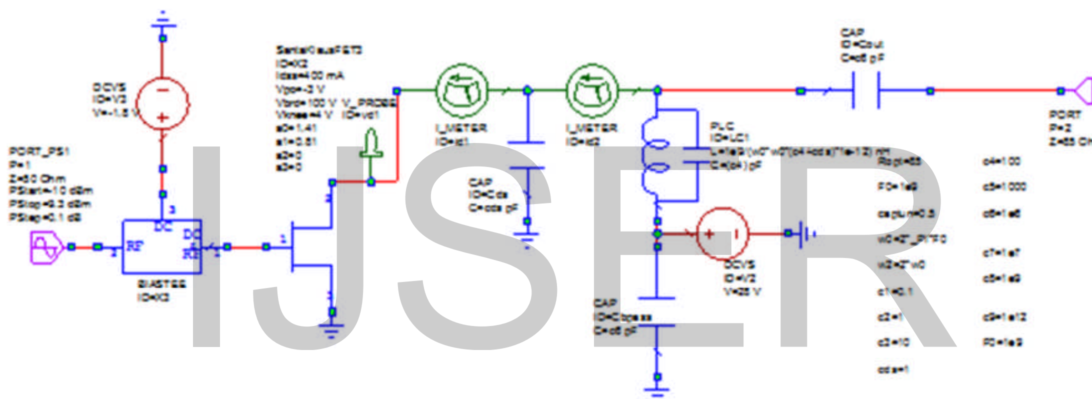

IJSER

Figure 4.19: Class B RFPA implemented considering the transistor parasitic, C_{DS}, using Bypass capacitor and output capacitor (without a biastee)

Exemplified in figure 4.20, shows the comparison plots of the drain efficiency, output power and the power gain of the configurations of the both Class B networks (figure 4.16 and figure 4.19). Also, tabulated in table are some selected choices of capacitors and inductors that can be used for the resonance circuit to obtain optimum performance as per the simulations performed during this project. Thus, in using and ideal or mathematical model for design works, technique of such is necessary to be performed so as to obtain optimum design goals.

- 56 -

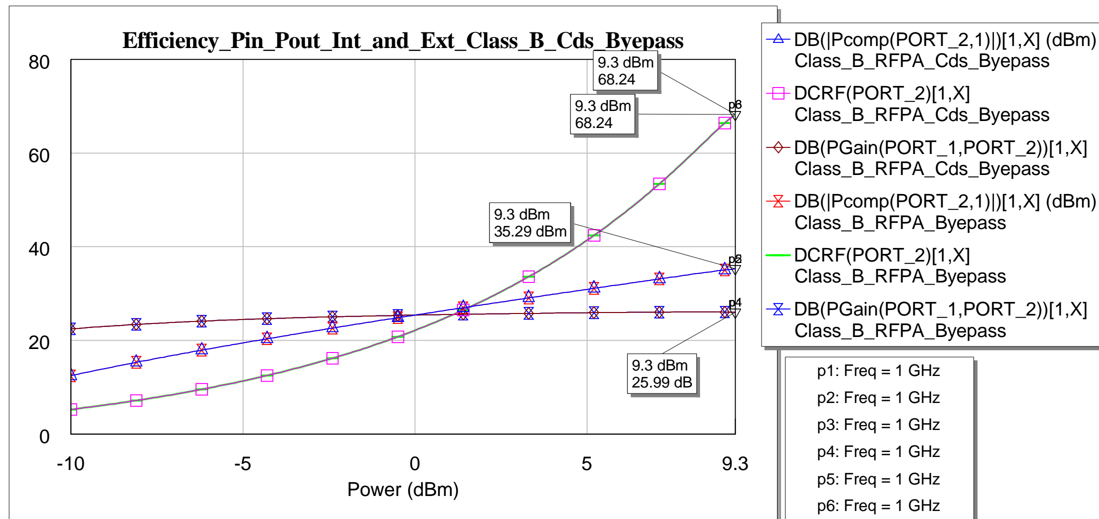

Figure 20: Drain efficiency and output power comparison of Class B RFPA consideration with and without parasitic – circuits with Byepass capacitor configuration.

IJSER

Table 4.4: Selected components values for implementing Class B RFPA considering transistor parasitic using real resonators, byepass capacitor and output capacitor					
Family A		Family B		Family C	
C_{LC}(pF)	0.1	C_{LC} (pF)	1	C_{LC} (pF)	10
L_{LC}(nH)	23.03	L_{LC} (nH)	12.66	L_{LC} (nH)	2.303
C_{DS}	1	C_{DS}	1	C_{DS}	1
C_{BPASS}(pF)	10^6	C_{BPASS}(pF)	10^6	C_{BPASS}(pF)	10^6
C_{OUT}(pF)	10^6	C_{OUT}(pF)	10^6	C_{OUT}(pF)	10^6
η (%)	62.07	η (%)	64.07	η (%)	68.07
P_{OUT} (dBm)	34.6	P_{OUT} (dBm)	34.85	P_{OUT} (dBm)	35.27
I_{MAX}(mA)		I_{MAX}(mA)		I_{MAX}(mA)	
Family D					
C_{LC} (pF)	100				
L_{LC} (nH)	0.2508				
C_{DS}	1				
CBPASS(pF)	10^6				
C_{OUT}(pF)	10^6				
η (%)	68.28				
P_{OUT} (dBm)	35.29				
I_{MAX}(mA)					

CHAPTER FIVE

Conclusion

Considering market demands for Electronic Communication Technologies there are need for high efficiency RFPA for future enhancement for the Communication Industry. GaN HEMT appear to be one of the most promising technologies, especially due to its capability for reduce size, resulting in minor weight and parasitic effects. On the other side, circuit design scientific community has shown an increasing interest in the Class J RFPA: it derives from the Class B RFPA, and in particular its implementation with GaN can be made useful to achieved wider bandwidth RFPA. In this framework, this thesis work has started from the Class J waveforms analysis. In order to achieve this task, theoretical basis of the Class J have been exploited and Matlab was used to analyze the waveforms of the Class J. To prove the equivalence of the Class J to the Class B in terms of performances, and aiming at using electronic components to prove the reality of this emerging device, Microwave Office (MWO) simulations were performed starting with an ideal model and passing on to more real structures.

Finally, after performing these analysis and simulations, the Class J was proven to have similar drain efficiency and output power to that of the Class B.

IJSER

- 58 -

APPENDIX

In order to avoid error while running these codes, copy all the appendices into separate matlab file and place all the files into the same directory/folder, anyway the codes in appendix B can be run separately. This is done due to the file that contained the frequency spectrum function, appendix D.

Appendix A: Matlab codes for Class B RFPA

```
clear all
close all

% These codes generate Ideal drain current, voltage waveforms and power
% harmonics contents for class B RF power amplifier.

% teta=linspace(0,2*pi,1000);
% beta=linspace(-pi,2*pi,1000);
teta=0:pi/20:4*pi;
beta=-pi:pi/20:3*pi;

Vdc=0;
Nmax=1000;
m=0;
M=0;

% Drain Voltage (Vd)

Vd= Vdc+sin(beta);
figure, plot(teta/pi,(-1*Vd+1)/2,'r','linewidth',3);
title('Class B RFPA Ideal Voltage Waveforms','fontsize', 14)
grid on;
legend('DRAIN VOLTAGE');
xlabel('Angular Phase (\pi)','fontsize', 14);
ylabel('Drain Voltage (V)','fontsize', 14);

%Drain Current (Idhalf)

Idhalf=0;

for m=0:Nmax
m=M;
Idc=-1/pi;
Idharm=-2/pi/(m^2-1).*cos(m.*beta);
Idhalf=Idharm+Idhalf;
M=M+2;
end

Idfund=0.5*sin(beta);
Idhalf=pi*(Idc+Idfund+Idhalf);
figure, plot(teta/pi, Idhalf/3, 'b','linewidth',3);
```

IJSER

```
title('Class B RFPA Ideal Current Waveforms','fontsize', 14);
grid on;
legend('DRAIN CURRENT');
xlabel('Angular Phase, (\pi)','fontsize', 14);
ylabel('Drain Current (A)','fontsize', 14);

figure, plot(teta/pi,(-1*Vd+1)/2,'r',teta/pi, Idhalf/3, 'b','linewidth',3)
title('Figure 2.7: Class B RFPA Ideal Voltage and Current
Waveforms','fontsize', 18)
grid on;
legend ('Voltage', 'Current');
xlabel('Angular Phase (\pi)','fontsize', 18);
ylabel('Drain Votage (V): Drain Current (A)','fontsize', 18);

%%%%%%%%%%%%%%%%%%%%%%%%%%%%%%%%%%%%%%%%%%%%%%%%%%%%%%%%%%%%%%%%%%%%%%%%%%%
%%%%%%%%%%%%%%%%%%%%%%%%%%%%%%%%%%%%%%%%%%%%%%%%%%%%%%%%%%%%%%%%%%%%%%%%%%%
% Class B Output Power

Poutput=Vd.*Idhalf/2;
figure,plot(teta/pi,Poutput,'linewidth',3);
xlabel('Angular Phase (\pi)','fontsize', 14);
ylabel('Drain Power (watts)','fontsize', 14);
title('Class B RFPA Drain Power (Angular Phase)','fontsize', 14);
grid on;

% Class B Drain Power (V*I/2) Frequency response
% [YfreqDomain,frequencyRange] = frequency_spectrum(Poutput,length(Poutput));
[YfreqDomain,frequencyRange] = frequency_spectrum(Poutput,10);
centeredFFT4 = figure;

stem(frequencyRange,abs(YfreqDomain));
% figure,plot(frequencyRange,abs(YfreqDomain));

xlabel('Freq (Hz)','fontsize', 18);
ylabel('Amplitude','fontsize', 18);
title('Class B RFPA Drain Power Harmonic Contents, Using the CenteredFFT
Function',...
    'fontsize', 18);
grid on;
axis([-6,6,0,0.5]);
```

Appendix B: Matlab codes for Class J Continuum voltage Waveforms

```
clear all
close all
% In this case, the Class J drain voltage waveforms were generated from the
% general voltage waveform equation as mentioned by Cripps and also as
% exploited in [8].

% teta=linspace(0,2*pi,5000);
teta=linspace(0,4*pi,5000);
% teta=linspace(0,8*pi,5000);
 beta=1;
```

IJSER

- 60 -

```
alpha1=-1.05;
alpha2=-0.85;
alpha3=-0.65;
alpha4=-0.08;
alpha5=0.65;
alpha6=0.85;
alpha7=0.9;
alpha8=0.95;

alpha0=0;
alpha00=-1;
alpha01=-0.5;
alpha02=1;

% teta=0: 0.01*pi:6*pi;
% Ipeak=1;

Vdb=(1-beta*cos(teta));
Vd0=(1-alpha0*sin(teta));
Vd00=(1-alpha00*sin(teta));
Vd01=(1-alpha01*sin(teta));
Vd02=(1-alpha02*sin(teta));

Vd1=(1-alpha1*sin(teta));
Vd2=(1-alpha2*sin(teta));
Vd3=(1-alpha3*sin(teta));
Vd4=(1-alpha4*sin(teta));
Vd5=(1-alpha5*sin(teta));
Vd6=(1-alpha6*sin(teta));
Vd7=(1-alpha7*sin(teta));
Vd8=(1-alpha8*sin(teta));

Vdb1=Vdb.*Vd1;
Vdb2=Vdb.*Vd2;
Vdb3=Vdb.*Vd3;
Vdb4=Vdb.*Vd4;
Vdb5=Vdb.*Vd5;
Vdb6=Vdb.*Vd5;
Vdb7=Vdb.*Vd7;
Vdb8=Vdb.*Vd8;
Vdb0=Vdb.*Vd0;
Vdb00=Vdb.*Vd00;
Vdb01=Vdb.*Vd01;
Vdb02=Vdb.*Vd02;
hold on;
plot(teta/pi,Vdb1,'--b','linewidth',2);
plot(teta/pi,Vdb2,'--g','linewidth',2);
plot(teta/pi,Vdb3,'-c','linewidth',2);
plot(teta/pi,Vdb4,':y','linewidth',2);
plot(teta/pi,Vdb5,'--m','linewidth',6);
plot(teta/pi,Vdb6,'-k','linewidth',2);
plot(teta/pi,Vdb7,'-g','linewidth',2);
plot(teta/pi,Vdb8,'-b','linewidth',2);
plot(teta/pi,Vdb0,'-r','linewidth',2);
plot(teta/pi,Vdb00,'-m','linewidth',2);
plot(teta/pi,Vdb01,'-y','linewidth',2);
```

IJSER

```
plot(teta/pi,Vdb02,'--r','linewidth',2);
legend('\alpha=-1.05','\alpha=-0.85','\alpha=-0.65','\alpha=-
0.08','\alpha=0.65','\alpha=0.85',...
    '\alpha=0.9','\alpha=0.95','\alpha=0','\alpha=-1','\alpha=-
0.5','\alpha=1','fontsize',18);
grid on;

hold on;
title('Continuum voltage waveforms for Class J RFPA','fontsize', 18);
ylabel('Normalized Drain Voltage (V)','fontsize', 18);
xlabel('Angular Phase (\omega\tau), [radian]','fontsize', 18);
```

Appendix C: Matlab codes for Class J RFPA

```
clear all
close all

% Ideal drain current and voltage waveforms and power harmonic contents
% for class J power amplifier

% The Drain voltage in this cae was generated by manipulation of the Class
% B current waveform equation by shift it and find a desire amplitudes for
% the fundamental and second harmonic

Vdc=1;
% Ipeak=1;

% teta=linspace(0,4*pi,1000);
% teta=linspace(1,2*pi,1000);
 teta=0:pi/20:4*pi;

% Vd=Vdc+sqrt(2)*Vdc*sin(theeta+pi+pi/4)-0.5*Vdc*cos(2*theeta+pi-pi/2);

Vdfund=sqrt(2)*Vdc*sin(teta+pi+pi/4);
Vdsecharm=-0.5*Vdc*cos(2.*teta+pi/2);
Vd=Vdc+Vdfund+Vdsecharm;
figure,plot(teta/pi,Vd,'m','linewidth',4);
title('Class J RFPA Ideal Voltage Waveforms','fontsize', 18)
grid on;
legend('DRAIN VOLTAGE');
xlabel('Angular Phase (\pi)','fontsize', 18);
ylabel('Drain Voltage (V)','fontsize', 18);

%Class J Drain Current (Id):
% Id=1+(pi/2)*sin(teta)-(2/3)*(cos(2*theeta));

Idc=1;
Idfund=(pi/2)*sin(teta);
Idsecharm=-(2/3)*(cos(2*teta));
Id=Idc+Idfund+Idsecharm;
figure,plot(teta/pi,Id,'g','linewidth',4);
title('Class B RFPA Ideal Current Waveforms','fontsize', 18)
grid on;
```

IJSER

```
legend('DRAIN CURRENT');
xlabel('Angular Phase, (\pi)','fontsize', 18);
ylabel('Drain Current (A)','fontsize', 18);

figure,plot(teta,Vd,'m',teta,Id,'g','linewidth',4);
legend('DRAIN VOLTAGE','DRAIN CURRENT');
xlabel('Angular Phase (\pi)');
ylabel('Amplitude (Drain Voltage & Drain Current)');
title('Class J RFPA Ideal Voltage and Current Waveforms','fontsize', 18)
grid on;
legend ('Drain Voltage', 'Drain Current','fontsize', 18);
xlabel('Angular Phase (\pi)','fontsize', 18);
ylabel('Drain Votage (V) & Drain Current (A)','fontsize', 14);


%%%%%%%%%%%%%%%%%%%%%%%%%%%%%%%%%%%%%%%%%%%%%%%%%%%%%%%%%%%%%%%%%%%%%%%%%%%
%%%%%%%%%%%%%%%%%%%%%%%%%%%%%%%%%%%%%%%%%%%%%%%%%%%%%%%%%%%%%%%%%%%%%%%%%%%

% Class J Drain Power (V*I/2) Frequency response

Poutput=Vd.*Id/2;
% Poutput=((Vd).^2)/(Zoutput)/2;
figure,plot(teta/pi,Poutput);
xlabel('Angular Phase (\pi)','fontsize', 14)
ylabel('Drain Power (watts)','fontsize', 14)
title('Class J RFPA Drain Power (Angular Phase)','fontsize', 14)
grid on;

% Class J Drain Power (V*I/2) Frequency response

% [YfreqDomain,frequencyRange] = frequency_spectrum(Poutput,length(Poutput));
[YfreqDomain,frequencyRange] = frequency_spectrum(Poutput,10);
centeredFFT4 = figure;

stem(frequencyRange,abs(YfreqDomain));
% figure,plot(frequencyRange,abs(YfreqDomain));

xlabel('Freq (Hz)','fontsize', 18)
ylabel('Amplitude','fontsize', 18)
title('Class J RFPA Drain Power Harmonic Contents, Using the CenteredFFT
Function',...
'fontsize', 18)
grid on;
axis([-6,6,0,0.15]);
```

IJSER

Appendix D: Matlab codes for frequency spectrum

```
function [X,freq]=frequency_spectrum(x,Fs)
%this is a custom function that helps in plotting the two-sided spectrum
%x is the signal that is to be transformed
%Fs is the sampling rate
 N=length(x);

%this part of the code generates that frequency axis
```

- 63 -

```
if mod(N,2)==0
    k=-N/2:N/2-1; % N even
else
    k=-(N-1)/2:(N-1)/2; % N odd
end
T=N/Fs;
% T=N/1000000000
freq=k/T;  %the frequency axis

%takes the fft of the signal, and adjusts the amplitude accordingly
X=fft(x)/N; % normalize the data
X=fftshift(X); %shifts the fft data so that it is centered
```

IJSER

- 64 -

REFERENCES

[1] Maas, Stephen A, Nonlinear microwave and RF circuits, 2nd edition, Artech house microwave library

[2] Cripps, Steve C. RF power amplifiers for wireless communications, 2nd ed, Artech House microwave library

[3] http://en.wikipedia.org/wiki/Electronic_amplifier

[4] Inder J Bahl, Fundamental of RF and Microwave Transistors Amplifiers, 2009, John Wiley & Sons Ltd

[5] Polito, Radio Frequency Design 2008/2009 Lecture Notes

[6] Franco Giannini and Giorgio Leuzzi, Nonlinear microwave circuit design, 2004, John Wiley & Sons Ltd,

[7] Chris Roff, Jojannes Benedikt, Paul J. Tasker, Cardiff School of Engineering, Design Approach for Realization of Very High Efficiency Power Amplifiers, Cardiff University, Cardiff, Uk, 2007

[8] Steve C. Cripps, Class J theory and concepts, ECI-Europe AB, 2010

[9] Steve C. Cripps, Paul J. Tasker, Alan L. Clarke, Jonathan Lees, and Johannes Benedikt, On the Continuity of High Efficiency Modes in Linear RF Power Amplifiers, IEEE, 2009Kkkkkk

[10] Paolo Colantonio, Franco Giannini, Ernesto Limiti, Trends in High-Efficiency Power Amplifier Design Solutions

[11] T. Zhang, L.C.N de Vreede, E. Neo et al, Wideband Hybrid-Class Power Amplifier for Base Station Applications Using LDMOS with Envelope Tracking System, Delft University of Technology, July 2009

[12] NITRONEX Corporation, GaN Essentals: GaN for LDMOS Users, NITRONEX Corporation, June 2008

[13] **Y. Ando, Y.** Okamoto, T. Nakayama, T. Inoue, K. Hataya, H. Miyamoto, M. Senda, K. Hirata, M. Kosaki, N. Shibata, and **M.** Kuzuhara, **High Power AlGaN/GaN Heterojunction FETs for Base Station Applications,** ***R&D*** *Association for Future Electron Devices,Japan,*

[14] http://en.wikipedia.org/wiki/High_Electron_Mobility_Transistor

[15] Polito, Radio Frequency Devices 2008/2009 Lecture Notes

[16] F. Schwielz and O. Amhacher, Advances in GaN HEMT Development, Technische Universitat Ihnenau, Institut fir Festkorperelektronik, PF 100565,98684 Ilmenau, GermanyRecent, IEEE, 2003

[17] Steve C. Cripps, Paul J. Tasker, Alan L. Clarke, Jonathan Lees, and Johannes Benedikt, On the Continuity of High Efficiency Modes in Linear RF Power Amplifiers, IEEE, 2009

[18] Takashi Mimura, The Early History of the High Electron Mobility Transistor (HEMT), IEEE TRANSACTIONS ON MICROWAVE THEORY AND TECHNIQUES, VOL. 50, NO. 3, IEEE, MARCH 2002

[19] Umesh K. Mishra, Fellow IEEE, Likun Shen, Thomas E. Kazior, and Yi-Feng Wu, GaN-Based RF Power Devices and Amplifiers, IEEE, Vol. 96, No. 2, February 2008

IJSER